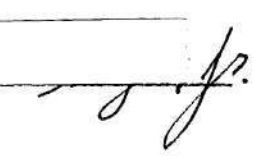


In presenting this dissertation as a partial fulfillment of the requirements for an advanced degree from the Georgia Institute of Technology, I agree that the Library of the Institute shall make it available for inspection and circulation in accordance with its regulations governing materials of this type. I agree that permission to copy from, or to publish from, this dissertation may be granted by the professor under whose direction it was written, or, in his absence, by the Dean of the Graduate Division when such copying or publication is solely for scholarly purposes and does not involve potential financial gain. It is understood that any copying from, or publication of, this dissertation which involves potential financial gain will not be allowed without written permission.

Hugh Elwyn Wingo Jr. 

THE HEAT TRANSFER COEFFICIENT FOR TRANSITION FLOW
IN A THERMAL ENTRANCE REGION OF UNIFORM WALL TEMPERATURE

A THESIS

Presented to
the Faculty of the Graduate Division
Georgia Institute of Technology

In Partial Fulfillment
of the Requirements for the Degree
Master of Science in Mechanical Engineering

By
Hugh Elwyn Wingo, Jr.

September 1955

THE HEAT TRANSFER COEFFICIENT FOR TRANSITION FLOW
IN A THERMAL ENTRANCE REGION OF UNIFORM WALL TEMPERATURE

Approved:

Date Approved by Chairman: Sept. 29, 1955

ACKNOWLEDGEMENTS

I wish to express my sincere appreciation to Dr. W. B. Harrison, III, for his guiding interest and assistance. His ideas and advice have been exceedingly helpful in the preparation of this work. The comments and suggestions of Dr. M. J. Goglia and Dr. Clyde Orr, Jr., are also greatly appreciated.

TABLE OF CONTENTS

Chapter	Page
I. INTRODUCTION.	1
Entrance Region Phenomenon	
Previous Work	
Objective	
II. ANALYTICAL SOLUTIONS.	7
Laminar Flow	
Turbulent Flow	
III. DESCRIPTION OF THE APPARATUS.	15
General	
Calibration of the Thermocouples	
Assembly of the Heat Transfer Section	
Experimental Procedure	
IV. EXPERIMENTAL RESULTS.	21
General	
Examination of Experimental Conditions	
V. CONCLUSIONS AND RECOMMENDATIONS	25
VI. APPENDIXES	
A - Nomenclature.	28
B - Figures	30
C - Tables.	51
D - Sample Calculations	60
E - Examination of Heat Loss in Nylon Gaskets	62
F - Examination of Deviation of Wall Temperature in Heat Exchanger.	68
G - Error Analysis.	74
VII. BIBLIOGRAPHY.	79

LIST OF FIGURES

Figure	Page
1. Values of Constants for Equation 6.	31
2. Average Nusselt Number in Entrance Region of Uniform Wall Temperature.	32
3. Predicted Velocity Distribution, Turbulent Flow	33
4. Sketch of Apparatus	35
5. Photograph of Heat Transfer Section	37
6. Sketch of Heat Exchanger.	38
7. Sketch of Thermocouple Circuit.	39
8. Experimental Value of Average Nusselt Number in Entrance Region of Uniform Wall Temperature	40
9. Experimental Value of Average Nusselt Number in Entrance Region of Uniform Wall Temperature	42
10. Temperature Distribution in Heat Exchanger, Run No. 1	44
11. Figures Used in Gasket Analysis	45
12. Functions for Use in Gasket Analysis.	46
13. Temperature Distribution in Gasket.	47
14. Network for Heat Exchanger Analysis	48
15. Temperature Distribution in Heat Exchanger for Laminar Flow.	49
16. Temperature Distribution in Heat Exchanger for Turbulent Flow.	50

LIST OF TABLES

Table	Page
1. Calibration of Thermocouples	52
2. Tabulated Results	53
3. Original Data	56
4. Temperature Distribution in Heat Exchanger and Water Circuit, Run No. 1.	59

SUMMARY

The purpose of this investigation was to investigate fully developed flow in the transition region between laminar and turbulent flow in a thermal entrance region, to describe an experimental system to obtain pertinent information, and to compare analytical and experimental results.

A review of the literature was conducted as an introduction to the present investigation and showed that work had been done for laminar and for turbulent flow in a thermal entrance region. Special attention has been given to turbulent flow and many systems have used unique entrance shapes as well as fluids. This survey of the literature gave no indication that any work had been conducted on the transition region. This investigation is therefore intended to fill the void between laminar and turbulent flow in a thermal entrance region.

The analytical solutions used for this investigation were the Graetz solution for heat transfer from an isothermal wall to a fluid flowing in laminar motion. A solution for heat transfer from an isothermal wall to a fluid flowing in turbulent motion between flat plates was also used. This solution was based on that of Poppendiek and Palmer which they devised for describing the heat transfer to liquid metals. It was changed so as to describe the heat transfer to water.

An apparatus was described that is believed to be particularly suited to the investigation of heat transfer in an entrance region. The apparatus may be easily altered to permit use of any number of entrance configurations or heat exchange media. It was simple yet effective.

The only drawback seemed to be in the care necessary for assembling the apparatus correctly.

The experimental investigation consisted of obtaining heat transfer data to water flowing in small passages with the ratio of the length of the heater to the diameter of the heater equal to 0.475, 0.970, 1.38, and 2.12. The data were taken over a range of Reynolds number from 960 to 34,800, with heat transfer coefficients varying from $778 \frac{\text{Btu}}{\text{hr-ft}^2-\text{°F}}$ to $21,400 \frac{\text{Btu}}{\text{hr-ft}^2-\text{°F}}$ respectively.

Since a comparison was made between the analytical and experimental results, an analysis was conducted to ascertain how closely the experimental system adhered to the postulates of the analytical solutions. These were that: (1) longitudinal conduction is negligible compared to radial conduction, (2) heat is added to the fluid only in the heat exchanger, starting at $x = 0$ and continuing to $x = L$, and (3) the walls of the heat exchanger are isothermal. An examination of the first of these shows that longitudinal conduction may be neglected for water in this apparatus. An examination of the second postulate showed that the system in turbulent flow followed very closely the conditions of the analytical solutions. The system in laminar flow, however, permitted some 10 per cent of the total heat to be conducted into the water channel by the gaskets before and after the heat exchanger. An examination of the condition of isothermal walls showed that, in laminar flow, the experiments followed very closely the postulate of the analytical solution. The deviation of the wall temperature in turbulent flow, however, was found to be an average of 10.2 per cent of the difference between the first increment of the heat exchanger surface and the mean water temperature.

To estimate the other uncertainties of the apparatus, an error analysis was conducted and showed that a precision of about 20 per cent was had for the four heat exchanger sections when the results were plotted as Nusselt number versus Graetz number; about 24 per cent when the results were plotted as Nusselt number versus Reynolds number.

The conclusions from this investigation are that the results from the experiments in the laminar region cannot be compared to the analytical results because of excessive heat leakage to the water channel before and after the heat exchanger.

The results from the investigation in the turbulent region agree, within experimental error, to the analytical results.

The transition region begins at a Reynolds number of 1670. This is believed to be lower than the accepted value because the hydrodynamic calming section was too short to ensure a properly developed flow pattern.

The results of the four heat exchangers used could be represented by a single curve, beginning at a Graetz number of 200,000.

The rate of increase of the Nusselt number in the transition region depends on the $\frac{L}{D}$ ratio and is greatest for the smallest $\frac{L}{D}$ ratio.

Extremely high values of the heat transfer coefficient may be obtained in a thermal entrance region. Values up to three times the usual accepted long tube values were attained in this investigation.

The empirical equations presented by I. T. Aladyev, which conform to the experimental system, seem to yield values which are somewhat high. This is evidenced by the fact that his values are higher than the analytical and experimental results of this investigation.

The recommendations from this investigation are that a larger apparatus, similar to the one described, be used to investigate the transition region. This larger system would permit a smaller heat loss through the gaskets. A better method of assembling the apparatus should be devised so as to be sure a flawless tube is provided for the water channel.

CHAPTER I

INTRODUCTION

General.--The process of transferring heat between a pipe wall and a fluid flowing inside the pipe is widely used and much arduous study and work have contributed toward explaining the mechanisms present in such a system. One of the main problems is that of designing a heat exchanger that will transfer the most heat in the smallest space. One method of doing this would be to use effectively the thermal entrance region phenomenon in a heat exchanger. "A thermal entrance region results when a thermally established fluid flowing in a duct system suddenly flows over surfaces which possess some new temperature distribution." (1)¹ It is noted also that a thermal entrance region results when a fluid flowing in an adiabatic channel suddenly flows over surfaces which possess some new heat flux distribution. These two ideal cases have a discontinuity at $x = 0$ which gives rise to extremely large values of the heat transfer coefficient which can remarkably reduce the area necessary to transfer a given amount of heat. This may be illustrated by considering the definition of the heat transfer coefficient. Let $\frac{q}{A}$ be the heat flux across a solid-fluid interface. The fluid in contact with the wall will be in laminar motion if the fluid is not perfect. The mode of heat transfer through the fluid is then by molecular conduction only and

¹Numbers in parentheses refer to references in the bibliography.

therefore the following equation may be written for the heat transferred across the interface.

$$\frac{q}{A}\Big|_x = h_x(t_w - t_m)_x = -k \frac{\partial t}{\partial y}\Big|_{(x,0)} \quad (1)$$

In this case, x is measured from the beginning of the heated section along the interface, y is measured from the interface radially to a point in the fluid; k is the molecular thermal conductivity of the fluid, t_w is the wall temperature, and t_m is the mixed mean fluid temperature. By rearranging Equation 1, the heat transfer coefficient may be defined as

$$h_x = \frac{-k \frac{\partial t}{\partial y}\Big|_{(x,0)}}{(t_w - t_m)_x} \quad , \quad (2)$$

where the subscript x is used to denote that the values are dependent on the distance from the beginning of the heat section. It can be shown from Equation 2 for the case of a temperature discontinuity that if a fluid of uniform temperature, flowing in a passage of equal temperature, contacts a surface which has a new temperature at $x = 0$ and persists for all positive values of x , then as x approaches zero, $\frac{\partial t}{\partial y}(x, 0)$ approaches an infinite value. However, the value of $(t_w - t_m)_x$ is finite; therefore, h_x approaches an infinite value as x approaches zero. If, as in the case of a heat flux discontinuity, there is a new heat flux distribution at $x = 0$ which persists for all positive values of x , then it can be shown that $\frac{\partial t}{\partial y}(x, 0)$ is finite. However, the value of $(t_w - t_m)_x$ approaches zero as x approaches zero; therefore h_x possesses an infinite value as x approaches zero.

Thus we see that a heat exchanger which effectively used the thermal entrance region would require less area to transfer a given amount of heat than one which did not.

Previous Work.---The importance of the thermal entrance region has long been recognized and investigations as far back as 1885 are recorded when Graetz (2) derived a conduction solution for parabolic fluid flow in a tube with a uniform wall temperature entrance region. Stanton (3) in 1897 attempted to investigate the effect of pipe length on the heat transfer coefficient but was unable to draw any conclusions since he used pipes with ratios of $\frac{L}{D} = 31.6, 33.8, 41.6, \text{ and } 62.4$. The thermal entrance region does not appreciably affect the heat transfer coefficient for $\frac{L}{D}$ ratios over 30 or 40.

Nusselt (4) in 1917 used the data of Stanton (3) and Rietschel (5) with data of his own and proposed a method of taking into account the effect of thermal entrance region for the flow of gases by the following equation:²

$$Nu = 0.0362 Re^{0.8} Pr^{0.4} \left(\frac{L}{D} \right)^{-0.054} \quad (3)$$

Great strides were made in 1921 when Latzko (6) developed turbulent forced convection solutions for both hydrodynamic and thermal entrance regions with uniform wall temperature. He limited his solutions to systems in which the Prandtl number was equal to one and also where heat was transferred principally by eddy convection.

²See Appendix A for nomenclature.

Short heat exchangers were studied by Maryamov (7) in 1936 with special interest toward aircraft radiators. He attempted to determine the effect of the thermal and hydrodynamic entrance region on the heat transfer coefficient. He proposed the following equation which is more influenced by the $\frac{L}{D}$ ratio than that of Nusselt.

$$Nu = 0.25 \frac{D}{L} Re Pr \left[1 - 0.96 e^{-0.15 \frac{L}{D}} \right] \quad (4)$$

The next important contribution was thirteen years later when Sanders (8) developed turbulent flow convection solutions for uniform wall temperature entrance regions. He dealt only with fluids of high Prandtl number and solved the problem by transforming the turbulent core into a laminar core of equivalent thermal resistance.

Boelter, Young, and Iverson (9) investigated experimentally local heat transfer data for air flowing through a pipe with a uniform wall temperature entrance region. They used a series of hydrodynamic entrance conditions and a range of Reynolds number from 17,000 to 56,000.

Humble, Lowdermilk, and Grele (10) measured average heat transfer coefficients for air flow through a tube with a bellmouth entrance. By dividing the tube into 24 small sections, local heat transfer coefficients were calculated. Their data covered the range of Reynolds number from 5,000 to 250,000.

English and Barrett (11) measured local heat transfer coefficients for the case of mercury flowing in a nickel tube with uniform wall heat flux. They took data over a range of Reynolds number from 4,000 to 45,000 with their main interest focused on determining heat transfer

coefficients for tubes of $\frac{L}{D}$ ratio of 50, where the thermal entrance region does not appreciably affect the heat transfer coefficient. Their data could, however, be used to evaluate local values in the thermal entrance region for $\frac{L}{D}$ larger than 5.

Seban and Shimazaki (12) obtained numerical solutions for the thermal entrance region of uniform wall temperature by the finite differences method.

Poppendiek (13) developed the solutions for liquid metals flowing in a thermal entrance region of uniform temperature. He postulated low Prandtl number and turbulent flow that obeyed the one-seventh power law.

Aladyev (14) investigated experimentally the flow of water in a thermal entrance region. He recorded data in the range of Reynolds number of 2,500 to 100,000 and proposed the following equations for the average and local values of the heat transfer coefficient in tubes of $\frac{L}{D}$ less than 60:

$$Nu_{\bar{}} = 0.044 Re_{\bar{}}^{0.8} Pr_{\bar{}}^{0.4} \left(\frac{L}{D}\right)^{-2.25} Re_{\bar{}}^{-0.30} \quad (5)$$

$$Nu_L = C Re^N Pr^{0.4} \quad (6)$$

where C and N depend on the $\frac{L}{D}$ ratio and are found from Figure 1. The solution of Equation 6 for the average value of the Nusselt number is shown graphically on Figure 2.

Harrison (15) investigated both experimentally and analytically the flow of liquid metals, sodium and mercury, in a uniform wall temperature

thermal entrance region. He observed data in the range of Reynolds number of 20,000 to 200,000 and recommended extending the range to low Reynolds numbers of 1000 to 20,000 to investigate the influence of the change in velocity profile.

Deissler (16) investigated experimentally and analytically the turbulent flow of air in thermal entrance regions of tubes and pipes. He studied the effect of variable properties on the growth of the thermal and flow boundary layers as well as the effect of the initial velocity and temperature distribution.

These are the major studies on entrance regions, but we note that none dealt with flow in the transition region between laminar and turbulent motion of the fluid. An investigation of this nature would serve to clarify the effect of this change in velocity profile.

Objective.---It is therefore the objective of this thesis to investigate the fully developed flow of water in a thermal entrance region of uniform wall temperature in the range of Reynolds number from about 1,000 to 20,000; to describe an experimental system to obtain pertinent information, and to compare theoretical and experimental results.

CHAPTER II

ANALYTICAL SOLUTIONS

Laminar Flow.--The mathematical solution for heat transferred from a tube wall to a fluid flowing in streamline motion was first solved by Graetz (2) and is presented by Jakob (17). The local heat transfer coefficient may be defined as in Chapter I by

$$h_x = \frac{-k \left. \frac{\partial t}{\partial y} \right|_{(x,0)}}{(t_w - t_m)_x} \quad (2)$$

From Jakob, we see that

$$\begin{aligned} -k \left. \frac{\partial t}{\partial y} \right|_{(x,0)} &= \frac{k(t_o - t_w)}{r_w} \left[1.499 e^{-m_0 x} \right. \\ &\quad \left. + 1.078 e^{-m_1 x} + 0.358 e^{-m_2 x} + \dots \right], \end{aligned} \quad (7)$$

and that

$$\begin{aligned} t_w - t_m &= -(t_o - t_w) \left[0.820 e^{-m_0 x} \right. \\ &\quad \left. + 0.0972 e^{-m_1 x} + 0.0135 e^{-m_2 x} + \dots \right]. \end{aligned} \quad (8)$$

where the exponents are given by

$$m_n x = \frac{2 \beta_n^2}{G Z} \quad (9)$$

Values of β are:

$$\begin{aligned} \beta_0 &= 2.705 & \beta_1 &= 6.66 \\ \beta_2 &= 10.3 & \beta_3 &= 14.67^3 \end{aligned} \quad (10)$$

Combining Equations 7 and 8 gives

$$\begin{aligned} Nu_z = \frac{2 \left[1.499 e^{-2(2.705)^2/Gz} + 1.078 e^{-2(6.66)^2/Gz} \right.}{\left[0.820 e^{-2(2.705)^2/Gz} + 0.0972 e^{-2(6.66)^2/Gz} \right.} \\ \left. \left. + 0.358 e^{-2(10.3)^2/Gz} + \dots \right] \right.} \\ \left. + 0.0135 e^{-2(10.3)^2/Gz} + \dots \right]}. \end{aligned} \quad (11)$$

To calculate the average value of the Nusselt number over the length of the heat exchanger, Harrison (18) let

$$\begin{aligned} \psi = \left(0.820 e^{-2(2.705)^2/Gz} + 0.0972 e^{-2(6.66)^2/Gz} \right. \\ \left. + 0.0135 e^{-2(10.3)^2/Gz} + \dots \right), \end{aligned} \quad (12)$$

$$\begin{aligned} d\psi = - \frac{8}{Pe} \left(1.499 e^{-2(2.705)^2/Gz} + 1.078 e^{-2(6.66)^2/Gz} \right. \\ \left. + 0.358 e^{-2(10.3)^2/Gz} + \dots \right). \end{aligned} \quad (13)$$

³From a footnote in Jakob, page 453. Values up to β_{10} are given by J. Sellers, M. Tribus, and J. Klein, Heat Transfer to Laminar Flow in a Round Tube or Flat Conduit. . . The Graetz Problem Extended, A. S. M. E. Paper No. 55-SA-66, New York, New York, 1955.

From the definition,

$$Nu_L = \frac{D}{L} \int_0^{\frac{L}{D}} Nu_x d\left[\frac{L}{D}\right], \quad (14)$$

it is evident that

$$Nu_L = -\frac{1}{4} Gz \int_{\psi(0)}^{\psi(\frac{L}{D})} \frac{d\psi}{\psi}. \quad (15)$$

Thus,

$$Nu_L = -\frac{1}{4} Gz \ln \left[\frac{0.820 e^{-2(2.705)^2/Gz} + 0.0972 e^{-2(6.66)^2/Gz} + 0.0135 e^{-2(10.3)^2/Gz} + \dots}{0.820 + 0.0972 + 0.0135 + \dots} \right]. \quad (16)$$

It can be shown (19) that the denominator of Equation 16 is equal to one; therefore,

$$Nu_L = -\frac{1}{4} Gz \ln \left[0.820 e^{-2(2.705)^2/Gz} + 0.0972 e^{-2(6.66)^2/Gz} + 0.0135 e^{-2(10.3)^2/Gz} + \dots \right]. \quad (17)$$

Since the above solutions have not been evaluated for regions near a thermal entrance region, the solution of Leveque (20) may serve as an asymptotical solution to the solution of Graetz. Namely,

$$Nu_x = 1.0766 (Gz)^{\frac{1}{3}}. \quad (18)$$

Applying the definition of the value of the Nusselt number over the length of the tube, i.e., Equation 14, we obtain the following for Equation 18,

$$Nu_L = 1.615 (Gz)^{\frac{1}{3}}. \quad (19)$$

The solution of the above equations for the average values of Nusselt number is shown graphically on Figure 2.

Turbulent Flow.—Many solutions have been devised for the turbulent flow of fluid in a thermal entrance region. Almost all of these solutions have, however, been for fluids with Prandtl number equal to one or for fluids with low Peclet number. Therefore, a new solution to the problem will be used which is based on that of Poppendiek and Palmer (21) to describe the heat transfer to water in a thermal entrance region between flat plates. Since the thermal boundary layer is very thin, the results from this solution should compare very well to those for heat transfer to water in a thermal entrance region in circular pipes.

The differential equation for heat transfer from plate surfaces to a fluid may be written as:

$$u \frac{\partial t}{\partial x} = \alpha \frac{\partial^2 t}{\partial y^2}, \quad (20)$$

for a steady state, no heat generation condition. Let

$$u = B \left(\frac{y}{b} \right)^m. \quad (21)$$

Therefore,

$$B \left(\frac{y}{b} \right)^m \frac{\partial t}{\partial x} = \alpha \frac{\partial^2 t}{\partial y^2}. \quad (22)$$

From Poppendiek and Palmer (22),

$$\frac{t_w - t}{t_w - t_0} = \frac{\int_0^w \exp(-vw)^{m+2} dv}{\int_0^\infty \exp(-vw)^{m+2} dv}, \quad (23)$$

$$\frac{t_w - t}{t_w - t_0} = \frac{\int_0^w \exp(-vw)^{m+2} dv}{\Gamma\left(\frac{1}{m+2} + 1\right)},$$

where

$$w = y \left(\frac{B}{(m+2)^2 \alpha b^m \kappa} \right)^{\frac{1}{m+2}} \quad (24)$$

$$Nu_L = \frac{1}{\Gamma\left(\frac{1}{m+2} + 1\right)} \left[\frac{2^m B}{(m+2)^2} \left(\frac{D}{\nu} \right) \left(\frac{Pr D}{\kappa} \right) \right]^{\frac{1}{m+2}}. \quad (25)$$

It follows that

$$Nu_L = \frac{(m+2)}{(m+1) \Gamma\left(\frac{m+3}{m+2}\right)} \left[\frac{2^m B}{(m+2)^2} \left(\frac{D}{\nu} \right) \left(\frac{Pr D}{\kappa} \right) \right]^{\frac{1}{m+2}}. \quad (26)$$

To evaluate B, let

$$u^+ = \frac{u}{U \sqrt{\frac{f}{8}}}, \quad y^+ = \frac{y U \sqrt{\frac{f}{8}}}{\nu},$$

hence

$$u^+ U \sqrt{\frac{f}{8}} = B \left[\left(\frac{y^+}{b} \right) \left(\frac{1}{U \sqrt{\frac{f}{8}}} \right) \right]^m, \quad (27)$$

or

$$u^+ = \frac{B \left[\frac{1}{b U \sqrt{\frac{f}{8}}} \right]^m (y^+)^m}{U \sqrt{\frac{f}{8}}} = c (y^+)^m. \quad (28)$$

Therefore, the generalized velocity distribution will be represented by the expression

$$u^+ = c (y^+)^m \quad (28)$$

Thus,

$$B = \frac{c U \sqrt{\frac{f}{8}}}{\left[\frac{1}{b U \sqrt{\frac{f}{8}}} \right]^m} \quad (29)$$

$$B = \frac{c U \sqrt{\frac{f}{8}}}{2^m} \left[Re \sqrt{\frac{f}{8}} \right]^m.$$

From this,

$$Nu_l = \frac{m+2}{(m+1) \Gamma\left(\frac{m+3}{m+2}\right)} \left\{ \frac{2^m c U \sqrt{\frac{f}{8}} (Re \sqrt{\frac{f}{8}})^m}{(m+2)^2 2^m} \right\}^{\frac{1}{m+2}}$$

$$\left[\left(\frac{D}{\nu} \right) \left(\frac{Pr D}{\kappa} \right) \right] \right\}^{\frac{1}{m+2}}$$

or,

$$Nu_L = \frac{(m+2)}{(m+1)\Gamma(\frac{m+3}{m+2})} \left[\frac{C}{(m+2)^2} \left(Re \sqrt{\frac{f}{8}} \right)^{m+1} \left(\frac{Pr D}{\nu} \right) \right]^{\frac{1}{m+2}}$$

Finally,

$$\frac{Nu_L}{\left[Pr \frac{D}{L} \right]^{\frac{1}{m+2}}} = \frac{m+2}{(m+1)\Gamma(\frac{m+3}{m+2})} \left[\frac{C}{(m+2)^2} \right]^{\frac{1}{m+2}} \left(Re \sqrt{\frac{f}{8}} \right)^{\frac{m+1}{m+2}} \quad (30)$$

To evaluate the thickness of the thermal boundary layer, let

$$w = y \left(\frac{B}{(m+2)^2 \propto b^m \nu} \right)^{\frac{1}{m+2}} \quad (24)$$

$$w = y \left[\frac{C U \sqrt{\frac{f}{8}} (Re)^m \left(\sqrt{\frac{f}{8}} \right)^m}{(m+2)^2 \propto b^m \nu} \right]^{\frac{1}{m+2}} \quad (31)$$

or,

$$w = \frac{y}{D} \left[\frac{2^m C}{(m+2)^2} \left(Re \sqrt{\frac{f}{8}} \right)^{m+1} \left(\frac{Pr D}{\nu} \right) \right]^{\frac{1}{m+2}} \quad (32)$$

Rearranging gives

$$\left[\frac{y}{D} \right]_{TBL} = w \left[\frac{(m+2)^2}{2^m C} \right]^{\frac{1}{m+2}} \frac{1}{\left(Re \sqrt{\frac{f}{8}} \right)^{\frac{m+1}{m+2}} \left(\frac{Pr D}{\nu} \right)^{\frac{1}{m+2}}} \quad (33)$$

In dimensionless form, this is expressed as

$$\frac{y}{D} \Big|_{TBL} = \frac{y^+}{Re \sqrt{\frac{f}{8}}} \quad (34)$$

The problem of obtaining the constants in Equation 30 is solved by fitting the postulated equation for the velocity distribution to that of the generalized velocity distribution as shown on Figure 3. If we assume the values of C and m in Equation 28 to have values of 1.38 and $3/4$ respectively, then from Equation 30,

$$\left(\frac{Nu}{Pr \frac{D}{L}} \right)^{\frac{4}{11}} = \frac{2.75}{1.5 \Gamma(\frac{15}{11})} \left[\frac{1.38}{(2.75)^2} \right]^{\frac{4}{11}} \left(Re \sqrt{\frac{f}{8}} \right)^{\frac{7}{11}},$$

$$Nu \Big|_L = 0.95 \left(Re \sqrt{\frac{f}{8}} \right)^{\frac{7}{11}} \left(Pr \frac{D}{L} \right)^{\frac{4}{11}}. \quad (35)$$

If we assume the values of C and m in Equation 28 to have values of 2.71 and $1/2$ respectively, then from Equation 30,

$$\left(\frac{Nu}{Pr \frac{D}{L}} \right)^{\frac{2}{3}} = \frac{2.5}{1.5 \Gamma(\frac{7}{3})} \left[\frac{2.71}{(2.5)^2} \right] \left(Re \sqrt{\frac{f}{8}} \right)^{\frac{3}{5}},$$

$$Nu \Big|_L = 1.345 \left(Re \sqrt{\frac{f}{8}} \right)^{\frac{3}{5}} \left(Pr \frac{D}{L} \right)^{\frac{2}{5}}. \quad (36)$$

The solutions of the above equations for the average value of Nusselt number are shown graphically on Figure 2.

CHAPTER III

DESCRIPTION OF APPARATUS

General.--The apparatus was patterned, though not exactly, after the apparatus as used by Harrison (15). The over-all apparatus is shown in Figure 4 by a schematic diagram, and the heat transfer section is shown in Figure 5 by a photograph. The apparatus consisted of (1) water pressure reducing and regulating valves, (2) a heat transfer section, (3) a temperature measuring system, (4) an electrical regulating and measuring system, (5) a flow measuring system, and (6) the necessary piping and pressure gauges. The construction and function of each of these principal components will be discussed in detail below.

The water used as the heat transfer medium was controlled principally by a Climax Controls, type 215L, variable pressure reducing valve. At the low range of the data taken, the back pressure valve, a $\frac{1}{2}$ in. Nibco No. 80 globe valve, was closed to throttle the flow so that accurate temperature measurements in the water system could be made. The temperature of the water in and out of the heat exchanger was measured by thermocouples placed in thermowells and attached to the main flow channel by standard $1/4$ in. pipe tees. When the flow was in the range of a Reynolds number of 1,000 to 3,000, the pipe tees were not sufficiently flooded to submerge the thermocouple junctions. Thus, the temperature of the water could not be measured accurately; however, throttling the flow by the back pressure valve permitted the thermocouple junctions to be submerged and hence alleviated the difficulty. To direct the flow

from the drain line into the flow measuring system, a standard 1/4 in. three-way valve was used. The water was turned 90° from its normal passage when the three-way valve was placed in position 2, the measuring position. This resulted in a larger pressure drop than was caused by the valve in position 1. When in position 2, the flow was altered and caused the temperatures in the heat exchanger to change from their value at steady state conditions, which were attained with the valve in position 1. To change this to a more favorable condition, a flow adjusting valve, a 1/4 in. Nibco No. 80 globe valve, was installed directly after the three-way valve. This valve was closed until there was no change in the temperatures in the heat exchanger as the valve was switched from position 1 to position 2.

The heat transfer section consisted of (1) mounting flanges, (2) hydraulic calming section, (3) heater and flange separator tube, (4) heat exchanger, and (5) a temperature sensing arrangement. These components will be discussed in detail below.

The mounting flanges were of stainless steel, tapped with standard 1/4 in. pipe threads to which the thermowells were attached, (Fig. 5). The hydraulic calming section was a stainless steel tube (0.25 in. to 0.375 in. outside diameter, 0.089 in. to 0.120 in. inside diameter) with an $\frac{L}{D}$ ratio of at least 30. The heater and flange separator tube was an exact duplicate of the hydraulic calming section. It served only to separate the heat exchanger from the flange so as to allow more area for insulation between these two components. The heat exchanger is shown in Figure 6. It may be considered to be a short thick-walled copper cylinder with a 3 in. outside diameter, 0.057 in. to 0.182 in. long,

0.089 in. to 0.120 in. inside diameter. A 1 in. wide copper rim was silver soldered to the periphery of the cylinder. A tubular inconel heater, manufactured by the Cromax Company of Buffalo, New York, with a 750 watt capacity was formed into a double circle and pressed snugly on the cylinder rim. These three pieces make up the heat exchanger. The temperature sensing arrangement consisted of number 30 constantan wires soldered in $1/64$ in. holes drilled in the copper cylinder as in Figure 6. A copper lead was soldered to the rim surface, permitting the cylinder itself to serve as a common copper lead to all constantan junctions. The leads were then passed to a terminal strip. The thermocouples for the temperature measurement of the water in and out of the heat transfer section were number 24 copper - constantan couples placed in thermowells, as in Figure 5. The leads were then passed to a terminal strip.

Leads were led from the terminal strips to a series of selector switches, as shown in Figure 7, to an ice point and then to a K-2 potentiometer, manufactured by Leeds and Northrup of Philadelphia, Pennsylvania. A Leeds and Northrup number 2430 D-C galvanometer was used with the potentiometer. The above comprised the temperature measuring system.

The electrical regulating and measuring system consisted of a Powerstat Variable Transformer, type 1226, manufactured by Superior Electric Company of Bristol, Connecticut, which adjusted the amount of current to the heater. This regulated current was measured by a single phase wattmeter, model 310, manufactured by Weston Electric Company of Newark, New Jersey.

The flow of water through the heat transfer section was determined by weighing the water during a given time interval. The water was weighed on a set of Toledo scales with a maximum capacity of 15 pounds, graduated in 1/100 of a pound. The time required for this weight of water to flow through the system was determined by the use of a Minerva stopwatch, graduated in 1/100 of a minute.

Calibration of the Thermocouples.--The thermocouples could not be calibrated after they had been installed in the heat exchanger. However, thermocouples from the same spool as those used in the heat exchanger and water circuit were calibrated against a standard thermometer by immersing the thermocouple junctions in a water bath which was heated by a Calrod electric heater. The water temperature was regulated by controlling the input to the heaters with a Variac transformer and the correct temperature of the water obtained from a nitrogen filled glass thermometer, calibrated by the U. S. Bureau of Standards to 0.1 of a degree Fahrenheit. Corrections for the stem temperature were applied to the thermometer readings and a temperature vs EMF curve for the copper-constantan thermocouples was prepared and used throughout the investigation for determining temperatures from the voltages read on the potentiometer. The method above yielded temperatures that were only slightly different from those as published by the U. S. Bureau of Standards, (23). The test results are given in Table I.

Assembly of the Heat Transfer Section.--Very meticulous care was taken when assembling the heat transfer section (Fig. 5) to assure that a flawless tube was provided for the water flow. This was extremely

important when the flow was laminar since the flow at the heat exchanger was postulated to be fully developed, i.e., at least beyond the thermal boundary layer. To do this, a drill rod of diameter no less than 0.002 smaller than the diameter of the water tube was threaded through the heat transfer section to align the components. The compression bolts were tightened and the system adjusted until the drill rod moved with ease through the heat transfer section. The passage was then visually inspected, after the drill rod had been removed. The thermowells were threaded into place on the flanges and the complete assembly then coupled to the piping provided. This was done for each of the four heat exchanger sections used. In order to insulate the heat exchanger to assure radial heat flow, the heat transfer section was placed in a corrugated box, 8 in. by 8 in. by 1¼ in., and the entire container filled with granular vermiculite. The thermocouple leads and heater wires were passed out the top of the box and joined to the terminal strips to complete the assembly of the apparatus.

Experimental Procedure.---At the beginning of each set of runs, the shut-off valve was opened to give pressure at the pressure reducer. If the data to be taken were in the range of Reynolds number of 1,000 to 3,000, the back pressure valve was almost completely closed in order to assure that the thermocouple junctions would be submerged in the thermowell arrangement. The pressure reducer was adjusted so that about 0.1 pound of water per minute was flowing through the system. The variable transformer was turned on and adjusted to give a temperature in the heat exchanger nearest the water tube of about 155° F. The system was then allowed to attain equilibrium. When equilibrium conditions were

established, the three-way valve was turned to position 2 at the same instant as the stop watch was started; the temperatures at two points for each of the four radial positions on the heat exchanger were recorded as well as the temperature of the water leaving the heat transfer section, and also the difference between the upstream and downstream water temperatures. The three-way valve was turned to position 1 and the stop watch halted. The water was weighed and the amount recorded with the time from the stop watch. This procedure was followed throughout the investigation except at the high flows. The back pressure valve was opened during the high flow rate and the flow adjusting valve was used to throttle the flow in order that the same pressure drop was had whether the three-way valve be in position 1 or 2. This being adjusted, the above procedure was then followed to obtain the data.

CHAPTER IV

EXPERIMENTAL RESULTS

The following data were observed and recorded in order that pertinent calculations could be made:

- (1) Water temperature downstream from the heat transfer section,
- (2) Water temperature difference between the water downstream and the water upstream from the heat transfer section,
- (3) Heat exchanger temperatures at two points for four different radial positions; eight readings total,
- (4) The weight of water that passed through the heat transfer section, and
- (5) The time required for the above amount of water to collect.

To insure that heat was not conducted from the heater to other parts of the apparatus by the connecting bolts, temperatures of the inlet and exit flanges as well as the calming tube and separator tube were taken. These temperatures were recorded at random throughout the investigation but were not used for any calculations. The operation of the apparatus was conducted as stated in Chapter III. Since the thermal conductivity of the copper heat exchanger varied less than one per cent, the rate of heat transfer and the temperature at the water-copper interface were calculated from

$$q = \frac{2\pi k L (t - t_w)}{\ln \frac{r}{b}}. \quad (37)$$

By arranging Equation 37, we obtain

$$t = t_w + \frac{q}{2\pi k L} \ln \frac{r}{b}. \quad (38)$$

From this we see that by plotting temperature at a given radius to the natural logarithm of the ratio of the given radius to the radius of the flow channel we have a linear relationship with a slope of $\frac{q}{2\pi k L}$ and an intercept of t_w . The averages of the upstream and downstream temperatures of the water were used as the mean temperature of the water in the heat exchanger. This mean temperature, together with the rate of heat transfer and the circumferential area, was used to compute the average heat transfer coefficient from the equation

$$h_L = \frac{q}{A(t_w - t_m)}, \quad (39)$$

where the subscript L denotes the average value over the length of the heat exchanger. The weight of water per unit time was used to obtain the Reynolds number from the equation

$$Re = \frac{4W}{\pi \mu D}. \quad (40)$$

A set of sample calculations is presented in Appendix D, showing the method of obtaining the results from the data for comparison with the analytical solutions. The results of these calculations are tabulated in Table II and are graphically represented in Figures 8 and 9. The original data taken are tabulated in Table III.

Since a comparison is made between the analytical solutions and the experimental results, it behooves the investigator to see how closely

the experimental system adheres to the conditions set forth in the analytical solutions. The major assumptions for the analytical solutions were that: (1) longitudinal conduction is negligible compared to radial conduction, (2) heat is added to the fluid only in the heat exchanger, starting at $x = 0$ and continuing to $x = L$, and (3) the walls of the heat exchanger are isothermal.

The first of these conditions was examined thoroughly by Harrison (24). His results show that the longitudinal conduction is negligible for Peclet number equal to or greater than 400. Since the lowest Peclet number observed in this investigation was 6,030, it is believed that longitudinal conduction can be neglected.

In order to examine the postulate that the heat leakage from the copper heat exchanger to the nylon gasket was negligible, an analysis was made of the heat conduction in the nylon gasket. This analysis is shown in Appendix E. The results show that the experimental system imposed conditions remarkably near those postulated for the analytical solutions in the turbulent flow region. For flow in the laminar region, it is noted that the heat leakage through the gasket was appreciable and resulted in the calculation of lower heat transfer coefficients by some 10 per cent since the temperature distribution in the heat exchanger was not a true indication of the amount of heat added to the fluid.

The analytical solutions with which the data are compared are based on the postulate of uniform wall temperature. To investigate the experimental system for variation in wall temperature, an analysis similar to the above was conducted as shown in Appendix E. The results of this inquiry show that for flow in the laminar region, the wall temperature

deviated only a negligible amount. For flow in the turbulent region, the deviation of wall temperature was found to be an average of 10.2 per cent of the difference between the first increment of the heat exchanger surface and the mean water temperature, based on one of the highest values of the heat transfer coefficients encountered during the experiments.

To evaluate other errors encountered during the experiments, an error analysis was made in Appendix H. The results from this analysis show that a precision of about 20 per cent was attained when the results for the four heat exchanger sections were plotted as Nusselt number versus Graetz number; about 24 per cent when the results were plotted as Nusselt number versus Reynolds number.

As shown in Table II, the heat transfer coefficients ranged from 778 $\frac{\text{Btu}}{\text{hr-ft}^2\text{-}^\circ\text{F}}$ to 21,400 $\frac{\text{Btu}}{\text{hr-ft}^2\text{-}^\circ\text{F}}$ for Reynolds numbers of 1,240 and 34,800 respectively. The region in which the data fell is shown on Figures 8 and 9. Although higher values of the heat transfer coefficient have been reached, the values from this investigation are exceedingly high for the Reynolds number used. This is borne out when one considers that the long tube value of the heat transfer coefficient to water for a Reynolds number of 34,800 for the same tube diameter as above is about 7,000 $\frac{\text{Btu}}{\text{hr-ft}^2\text{-}^\circ\text{F}}$. Thus, the values in a thermal entrance region for this case are three times the usual accepted long tube value.

CHAPTER V

CONCLUSIONS AND RECOMMENDATIONS

Conclusions.--As a result of the experiments which have been described, it is concluded that:

1. The results from the experiments in the laminar region were erratic since the temperature distribution in the heat exchanger was not a true representation of the rate of heat transfer to the water channel, as is shown in Appendix E. Therefore, no comparison can be made between the analytical and experimental results in this region.

2. The results from the experiments in the turbulent region agree, within experimental error, with the analytical solutions. The analytical solutions were based on the equations for heat transfer to a fluid flowing between flat plates, whereas the experimental arrangement was that of the transference of heat to a fluid inside a circular tube. It is concluded, however, that since the thermal boundary layer is very thin, the flat plate solution should conform exceedingly close to the circular tube solution.

3. The results from the experiments in the transition region between laminar and turbulent flow show that the trend in the thermal entrance region is to "break away" from the solution for the parabolic velocity distribution at a lower Reynolds number than usual. This may be caused by the hydrodynamic calming section being too short to ensure a properly developed flow pattern. This explanation seems reasonable

when one considers that the data show a Reynolds number of 1,670 to be the point at which the transition region begins for all the sections tested. It is noted that the results from all four heat exchangers could be represented by a single curve when the results were plotted as Nusselt number versus Graetz number, beginning at a Graetz number of 200,000.

4. The Nusselt number in the transition region rises rapidly as flow increases toward well established turbulent conditions. The rate of increase depends on the $\frac{L}{D}$ ratio and is greatest for the smallest $\frac{L}{D}$ ratio. In this investigation, the Nusselt number more than doubled for the heat exchanger with $\frac{L}{D} = 0.475$ as the Reynolds number increased from 2,000 to 3,000, while the increase in the Nusselt number for the heat exchanger with $\frac{L}{D} = 2.12$ was only 75 per cent of its value at the Reynolds number of 2,000.

5. Extremely high values of the heat transfer coefficient may be attained in the thermal entrance region. Although higher values of the heat transfer coefficient have been reached, the values from this investigation are exceedingly high for the Reynolds number used. This is borne out when one considers that the long tube value of the heat transfer coefficient to water for a Reynolds number of 34,800 is about 7,000 $\frac{Btu}{hr-ft^2-^{\circ}F}$ as compared to the value of 21,400 $\frac{Btu}{hr-ft^2-^{\circ}F}$ in the thermal entrance region for the same tube diameter. This value was obtained in this investigation for the thermal entrance region with $\frac{L}{D} = 0.475$. Thus, the values in this case are three times the usual accepted long tube values.

6. The apparatus described is considered to be very well suited for studying the effect of the thermal entrance region. This same apparatus may be easily modified to conform to a variety of entrance regions.

7. The empirical equations of I. T. Aladyev yield a value of the heat transfer coefficient that is considered to be somewhat higher than usual. The analytical solutions give results which are about 50 per cent lower than the results of Aladyev. The experimental results from this investigation give results which are about 30 per cent lower than the results of Aladyev. These examples tend to substantiate the belief that Aladyev's predictions are somewhat high.

Recommendations.--It is recommended that:

1. A larger apparatus, similar to the one described, should be used to investigate the heat transfer coefficient to fluid in laminar motion in a thermal entrance region. The larger system would permit a more accurate calculation of the heat transfer rate since more heat could be added to the water than in the present system. With more heat added, the heat loss through the gaskets would be negligible and the temperature distribution in the plate would then be an accurate measure of the rate of heat transfer to the water.

2. A better method of assembling the apparatus be devised to insure that there is no possibility of misalignment of the calming tube and gaskets. This is needed since a flawless calming section is imperative.

APPENDIX A

NOMENCLATURE

Latin Capital Letters.--

A	area, ft^2
B	constant
C	constant
D	equivalent diameter, or channel diameter, ft
L	channel length, ft
N	see Appendix F
P,S,T	see Appendix E
U	average fluid velocity, ft./sec.
W	flow rate, lb./sec.

Latin Lower Case Letters.--

b	radius, or half distance between plates, ft.
f	friction factor, or functional notation.
h	heat transfer coefficient, $\frac{\text{Btu}}{\text{hr-ft}^2\text{-}^\circ\text{F}}$
k	thermal conductivity, $\frac{\text{Btu}}{\text{hr-ft-}^\circ\text{F}}$
m	exponent
n	constant
q	heat transfer rate, Btu/hr
r	radius, ft.
t	temperature, $^\circ\text{F}$

u	velocity in x-direction, ft./sec.
w	term for describing thickness of thermal boundary layer
x, y, z	distance, ft.

Greek Letters.---

α	thermal diffusivity, ft. ² /hr.
β	value for determining exponent
Δ	an increment
T	Bessel function
μ	dynamic viscosity, lb./ft.-sec.
ν	kinetic viscosity, ft. ² /hr.
ψ	see Chapter II

Subscripts.---

L	average value over a length
m	condition at mean fluid property
o	initial condition, or conditions at origin of network unit
TBL	thermal boundary layer
w	conditions at the channel wall
x	local value

Dimensionless Moduli.---

G_z	Graetz, $\frac{4Wc}{\pi k L}$
N_u	Nusselt, $\frac{h D}{k}$
P_r	Prandtl, $\frac{c \mu}{k}$
R_e	Reynolds, $\frac{\rho D U}{\mu}$
u^+	$\frac{u}{U \sqrt{\frac{f}{8}}}$
y^+	$y \frac{U \sqrt{\frac{f}{8}}}{\nu}$

APPENDIX B

FIGURES

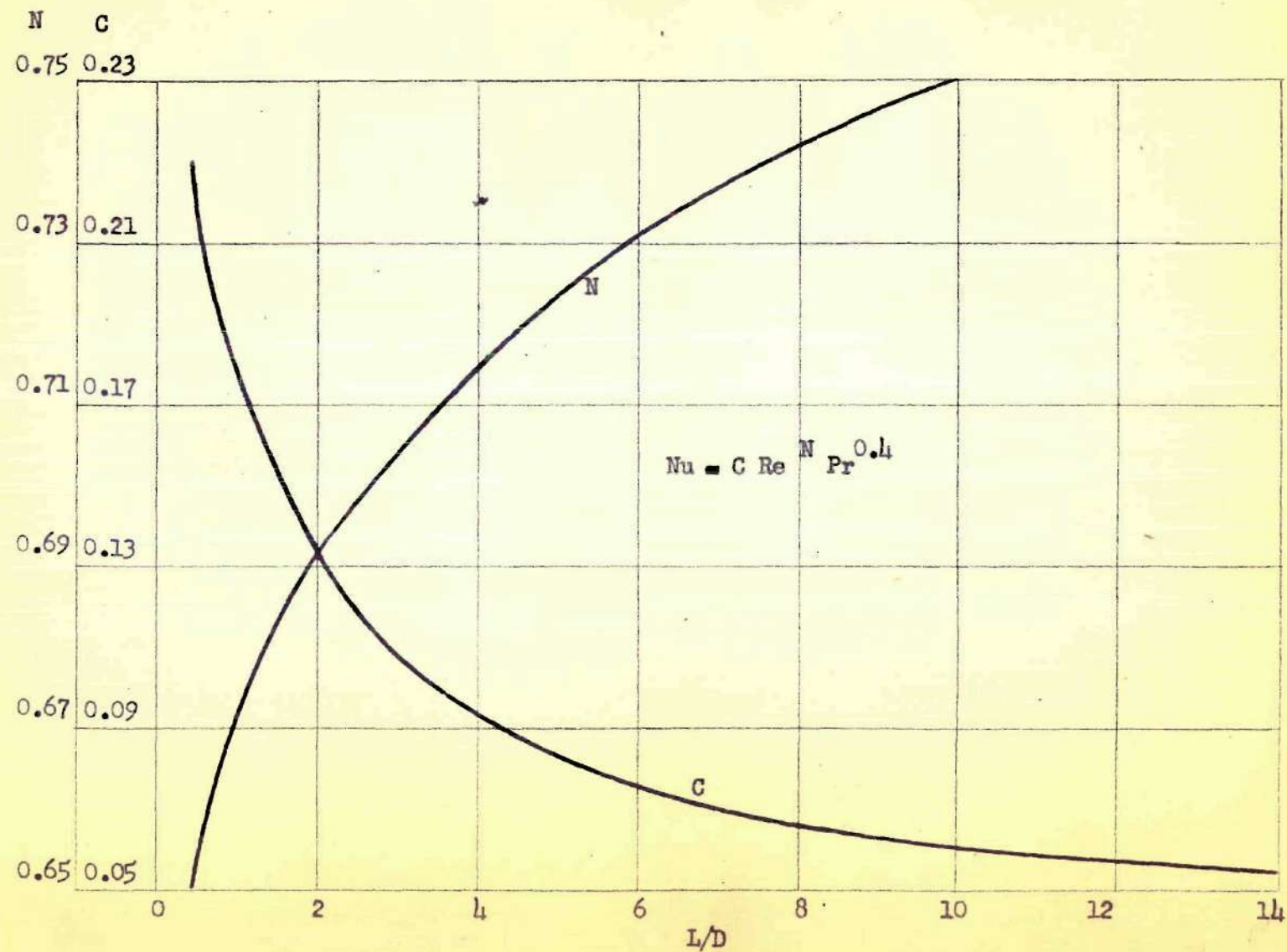


Fig. 1. Values of Constants for Use in Equation 6

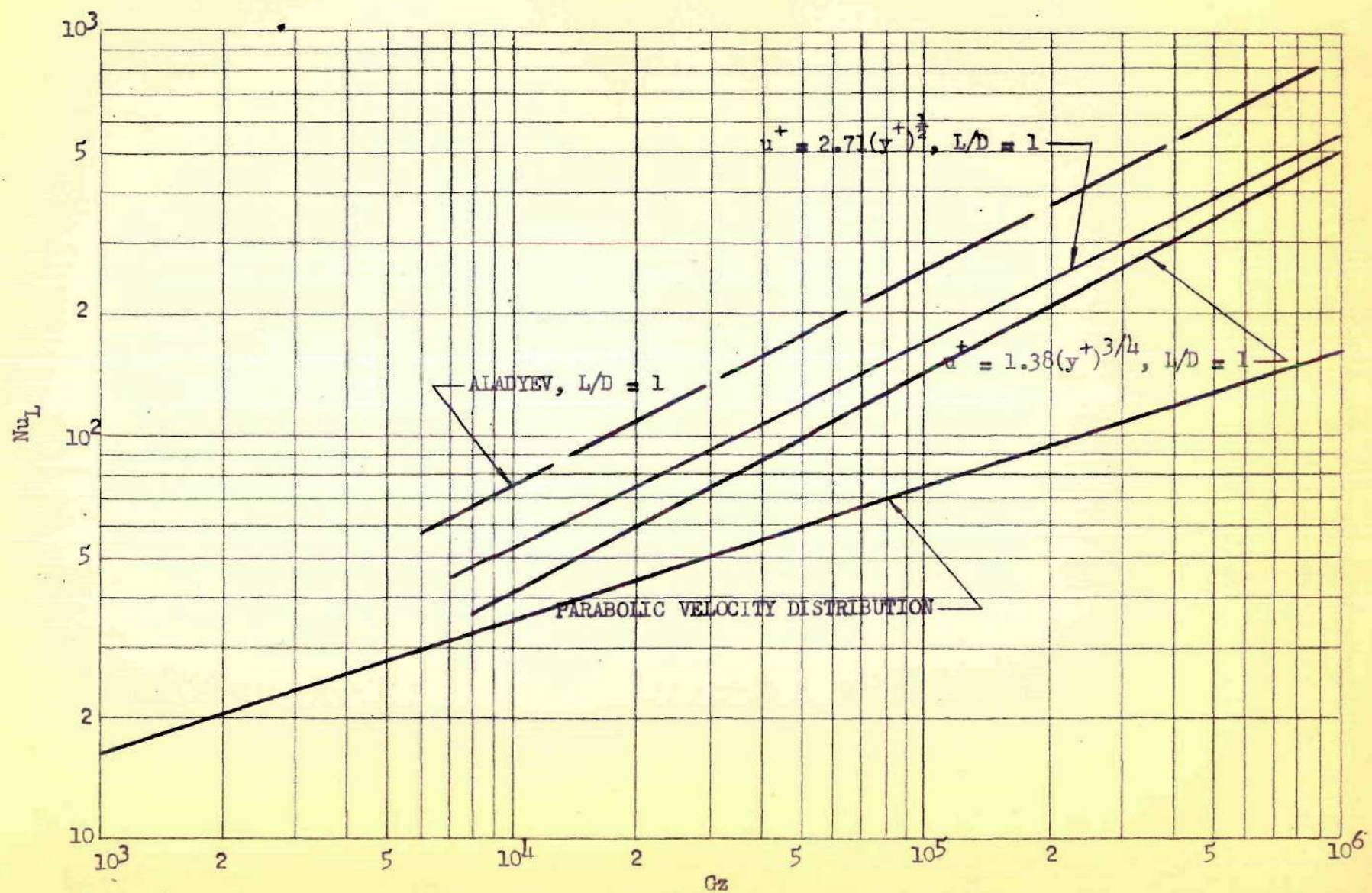


Fig. 2. Average Nusselt Number in Entrance Region of Uniform Wall Temperature

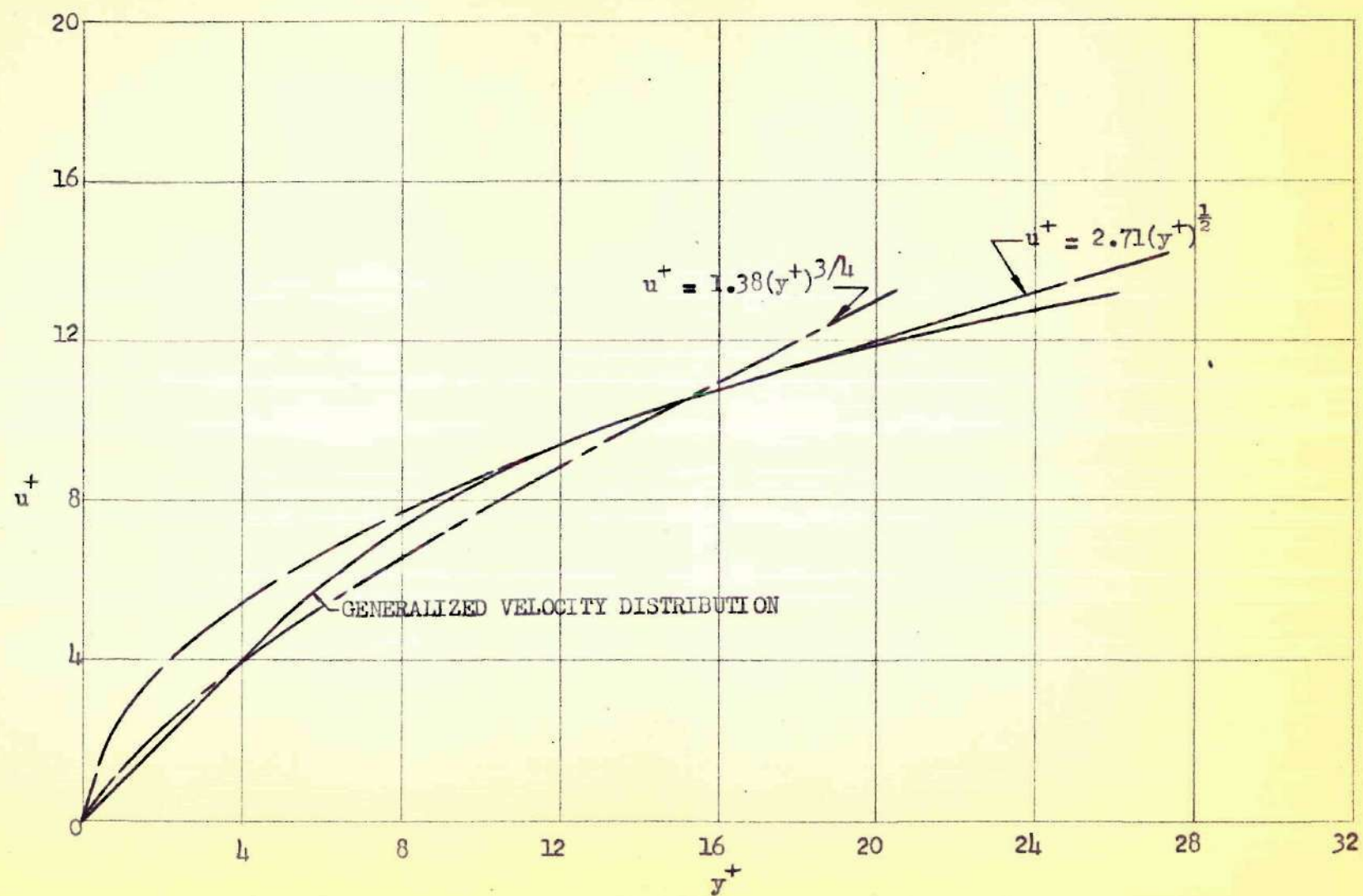


Fig. 3. Predicted Velocity Distribution, Turbulent Flow

KEY TO FIGURE 4

- A Variable Transformer
- B Wattmeter
- C Heat Transfer Section
- D Switch Panel
- E Potentiometer
- F Galvanometer
- G Shut-off Valve
- H Variable Pressure Reducer
- J Back Pressure Valve
- K Three-way Valve
- L Flow Adjusting Valve

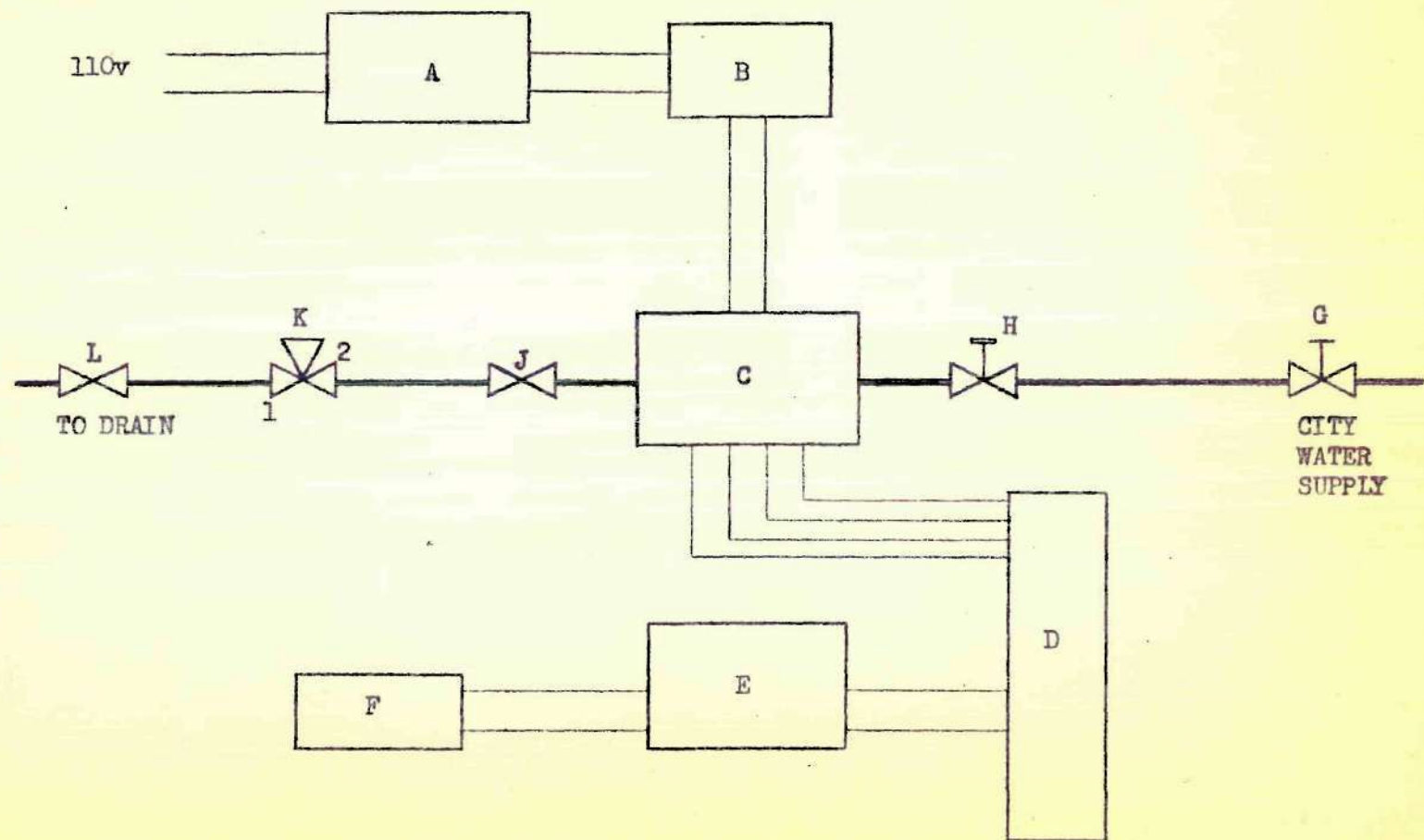


Fig. 4. Schematic Diagram of Apparatus

KEY TO FIGURE 5

- A Upstream Thermowell
- B Upstream Flange
- C Calming Section and Gaskets
- D Heat Exchanger
- E Separator Tube and Gaskets
- F Downstream Flange
- G Downstream Thermowell

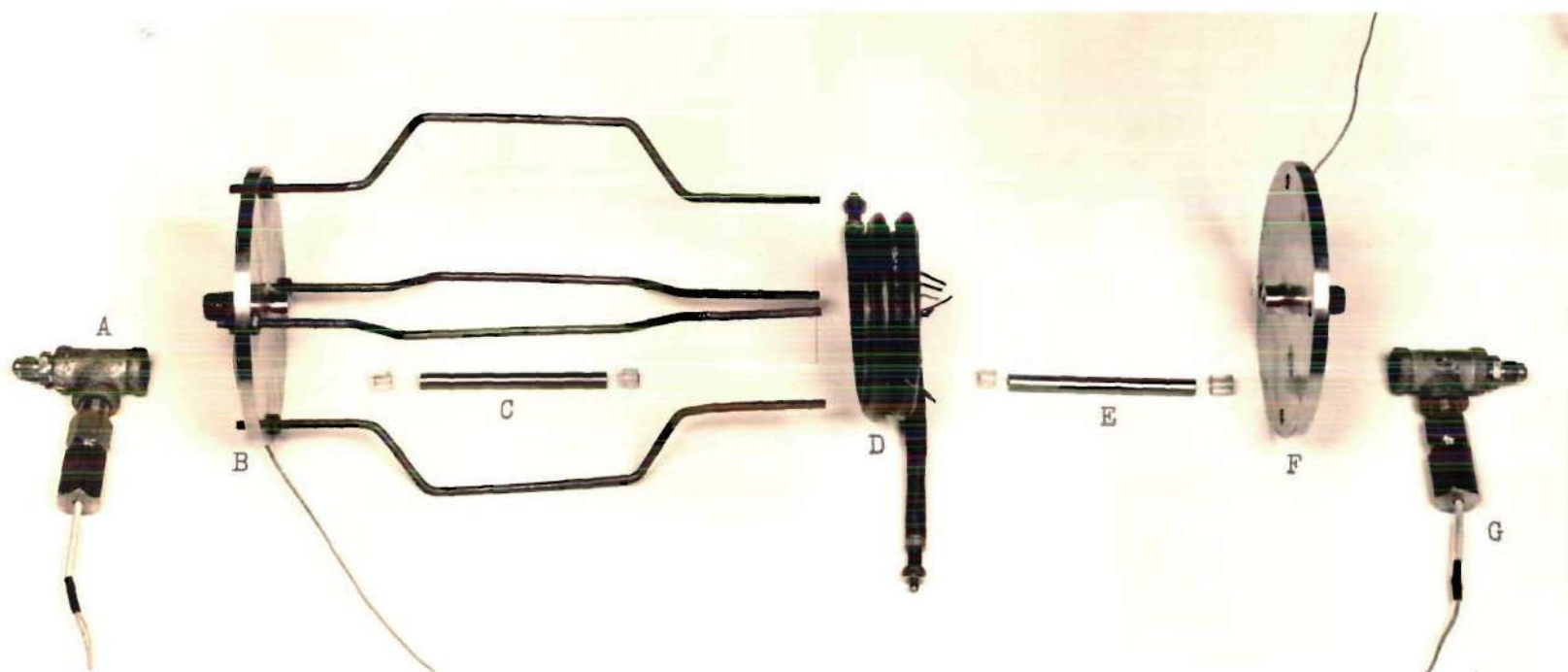


Fig. 5. Photograph of Heat Exchanger

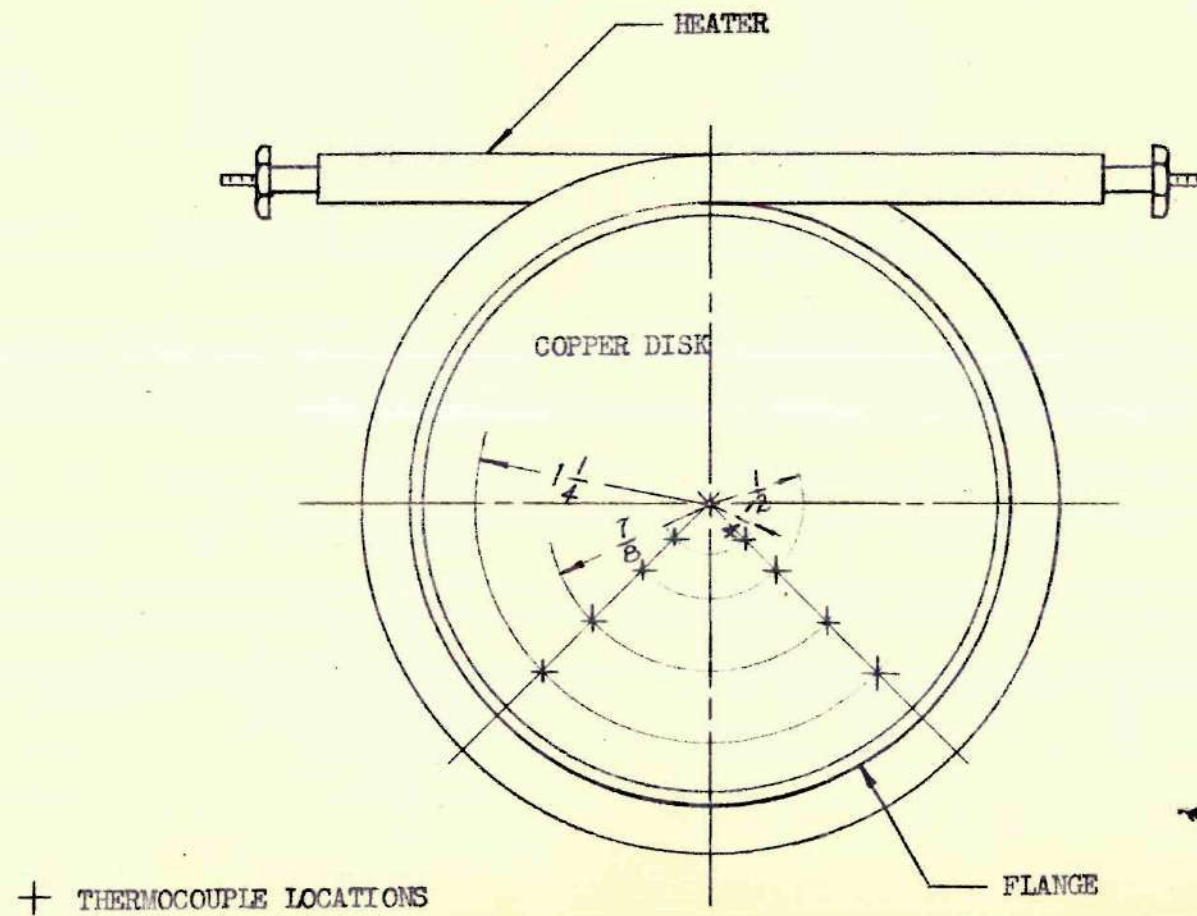


Fig. 6. Sketch of Heat Exchanger

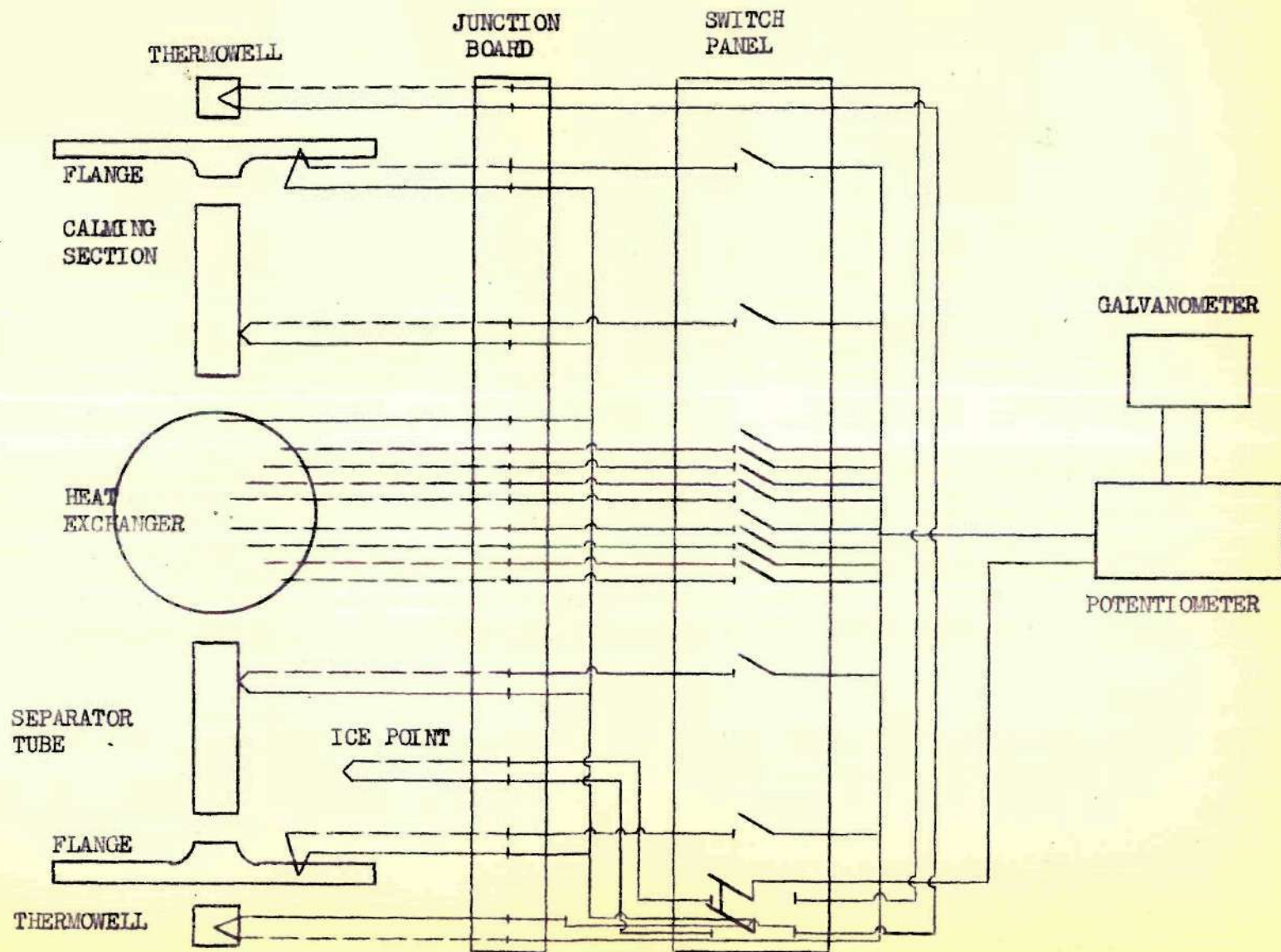


Fig. 7. Sketch of Thermocouple Circuit

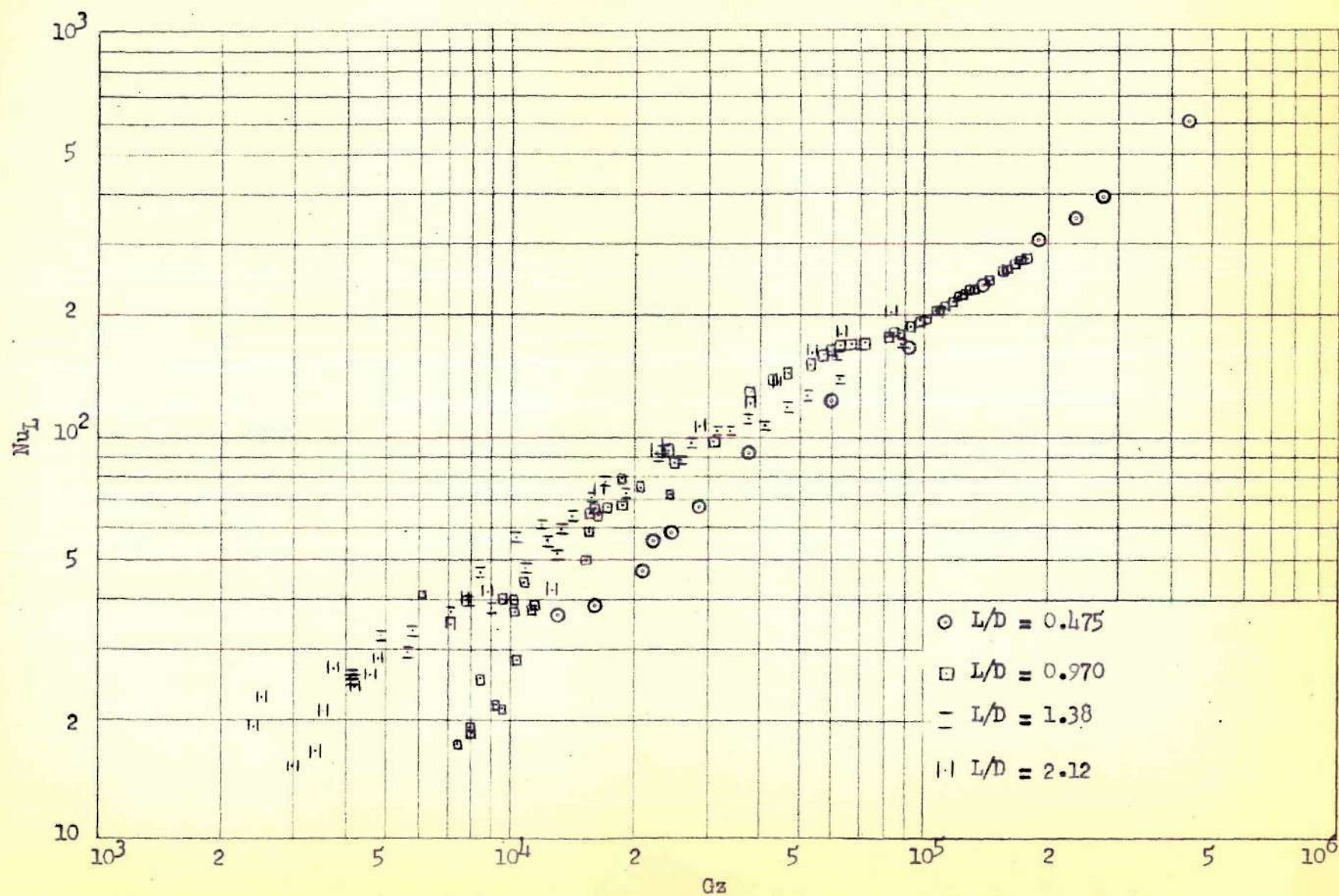


Fig. 8. Experimental Value of Average Nusselt Number in Entrance
Region of Uniform Wall Temperature
(Continued)

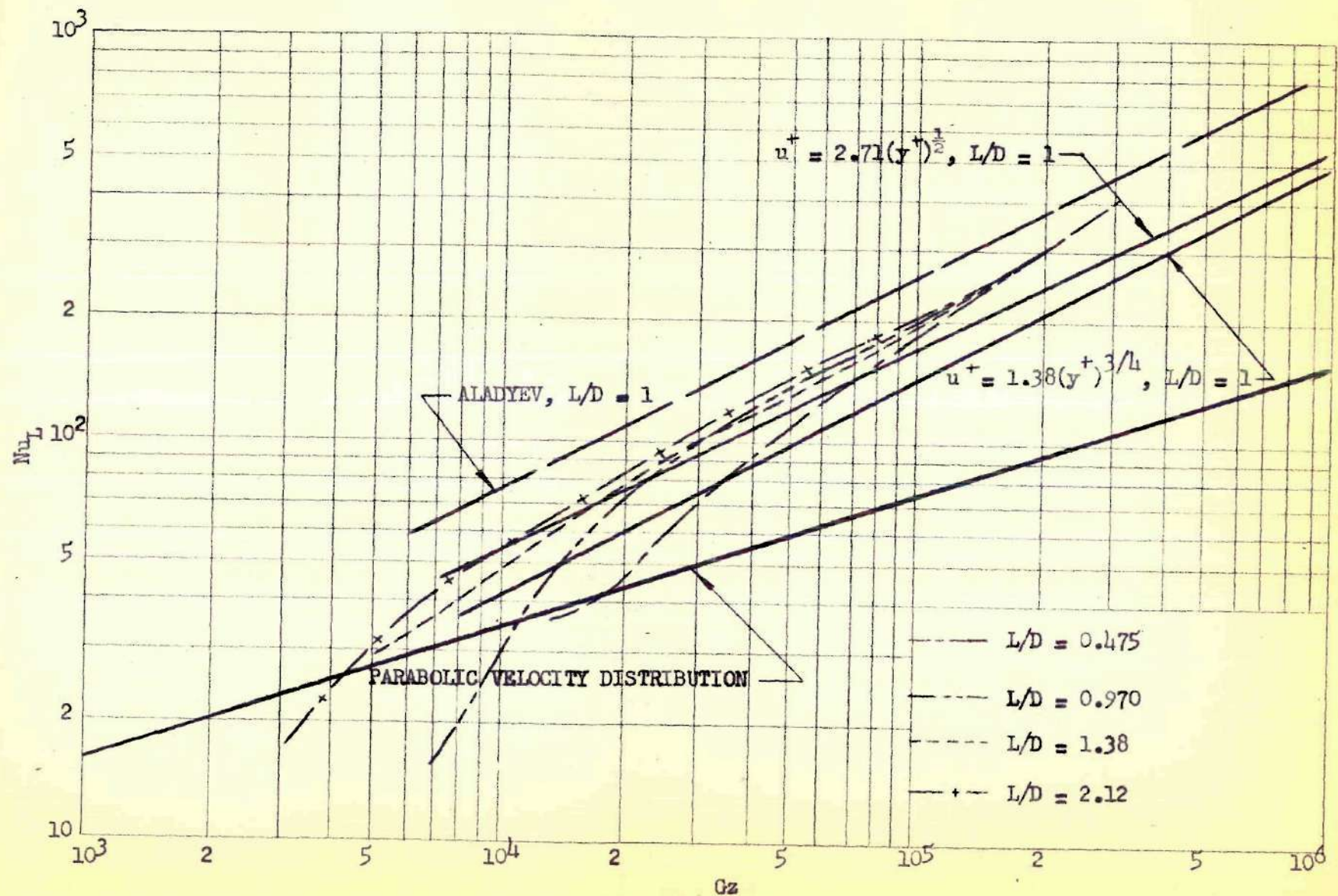


Fig. 8 (Continued). Experimental Value of Average Nusselt Number in Entrance Region of Uniform Wall Temperature

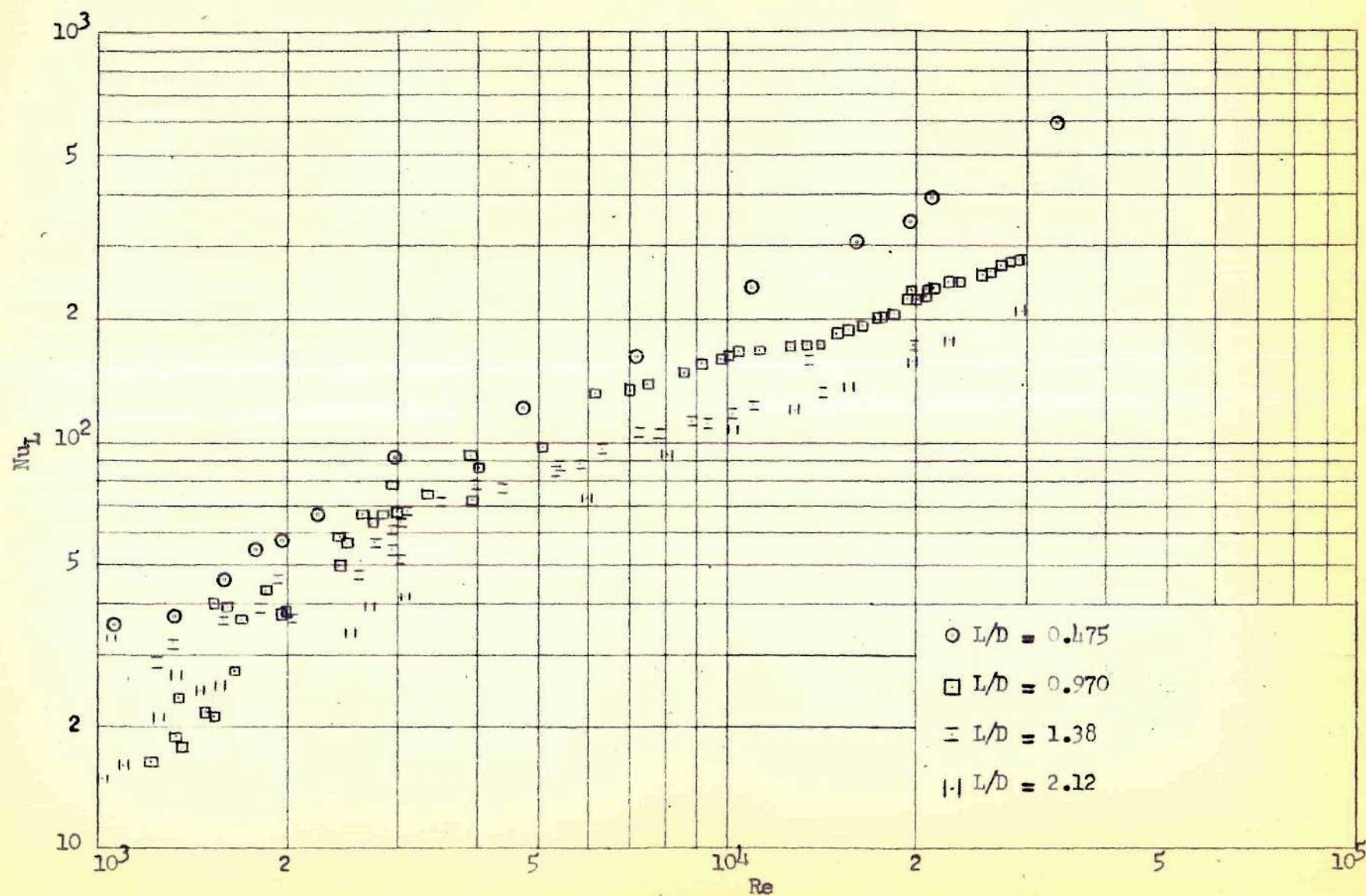


Fig. 9. Experimental Value of Average Nusselt Number in Entrance
Region of Uniform Wall Temperature
(Continued)

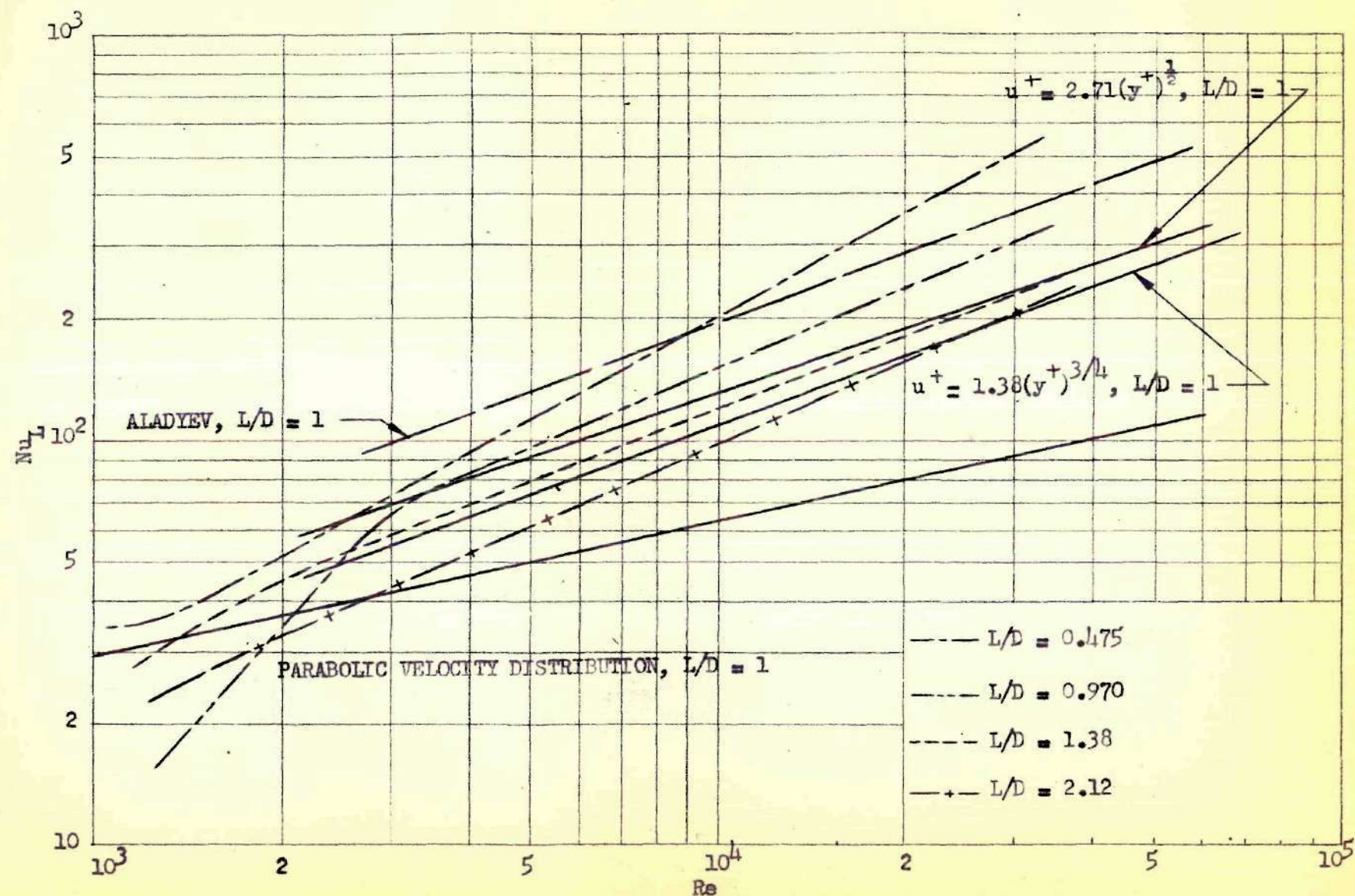


Fig. 9 (Continued). Experimental Value of Average Nusselt Number in Entrance Region of Uniform Wall Temperature

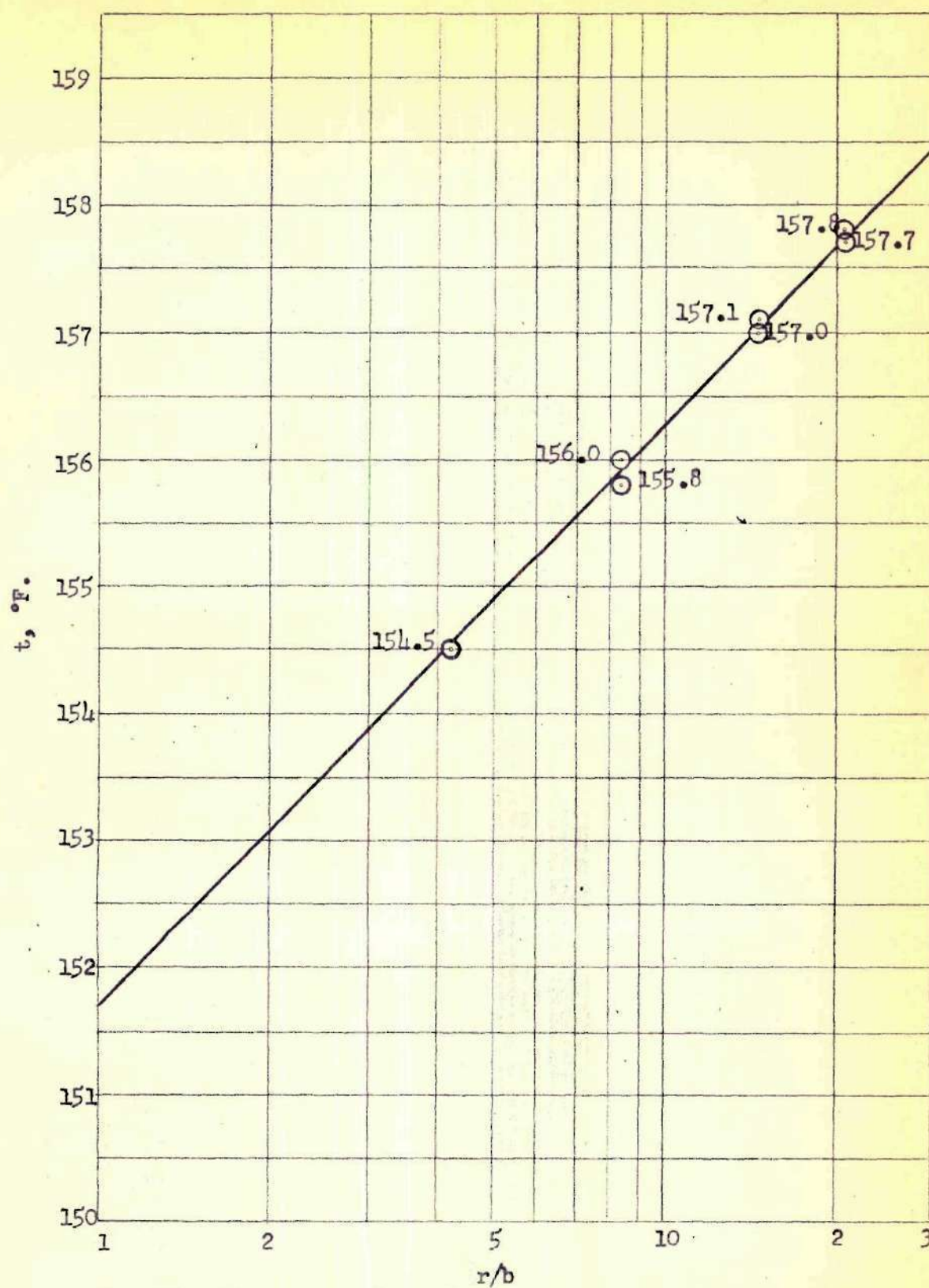
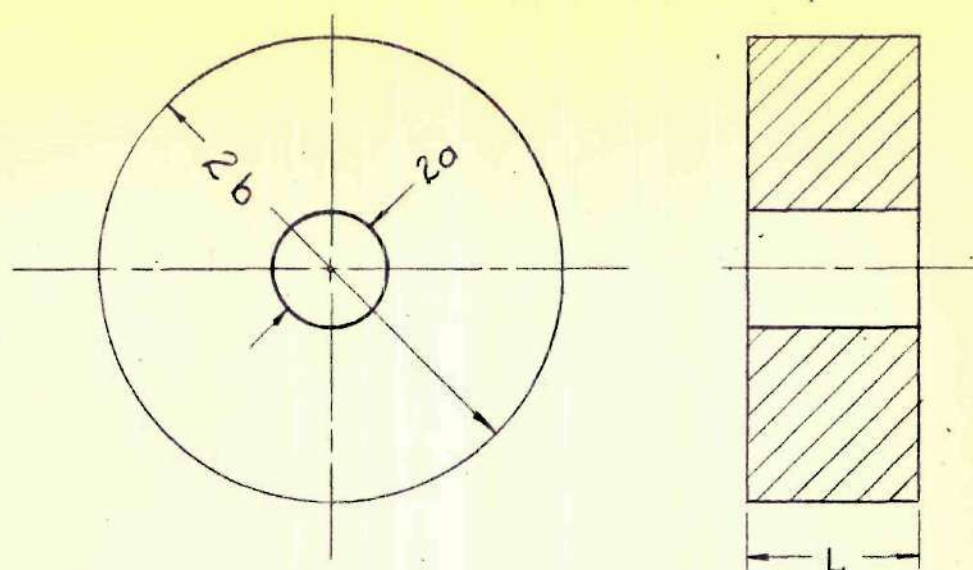
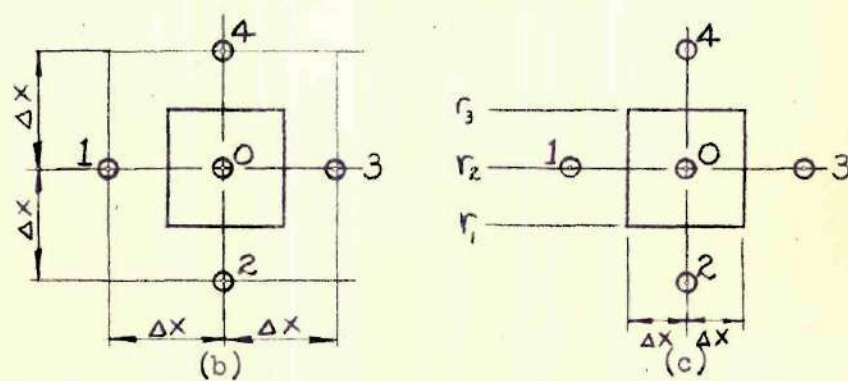


Fig. 10. Temperature Distribution in Heat Exchanger, Run No. 1

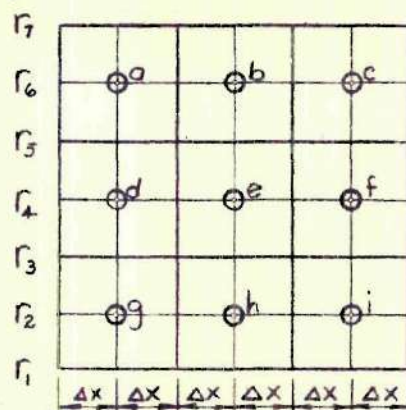


(a)



(b)

(c)



(d)

Fig. 11. Figures Used in Gasket Analysis

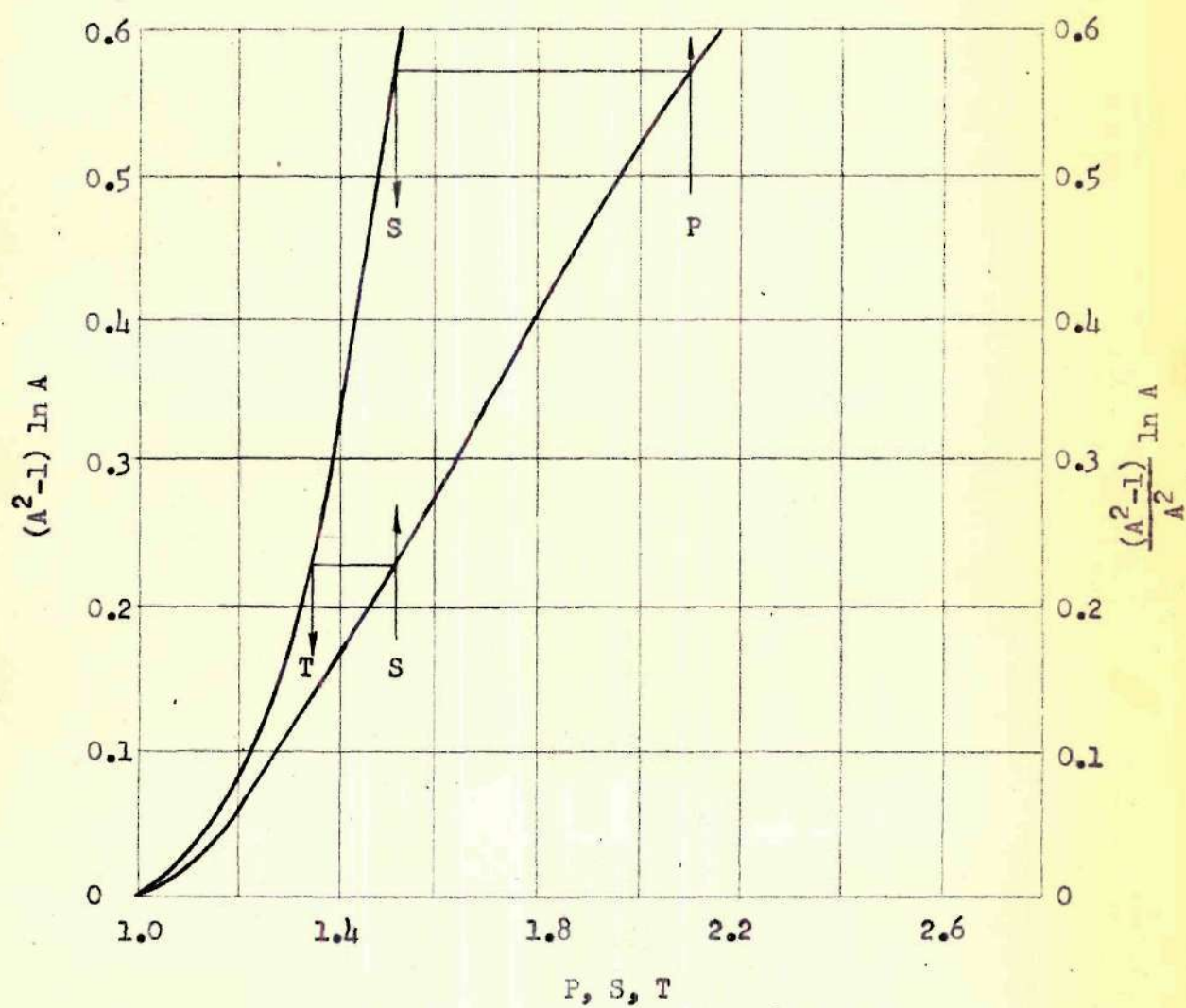


Fig. 12. Functions for Use in Gasket Analysis

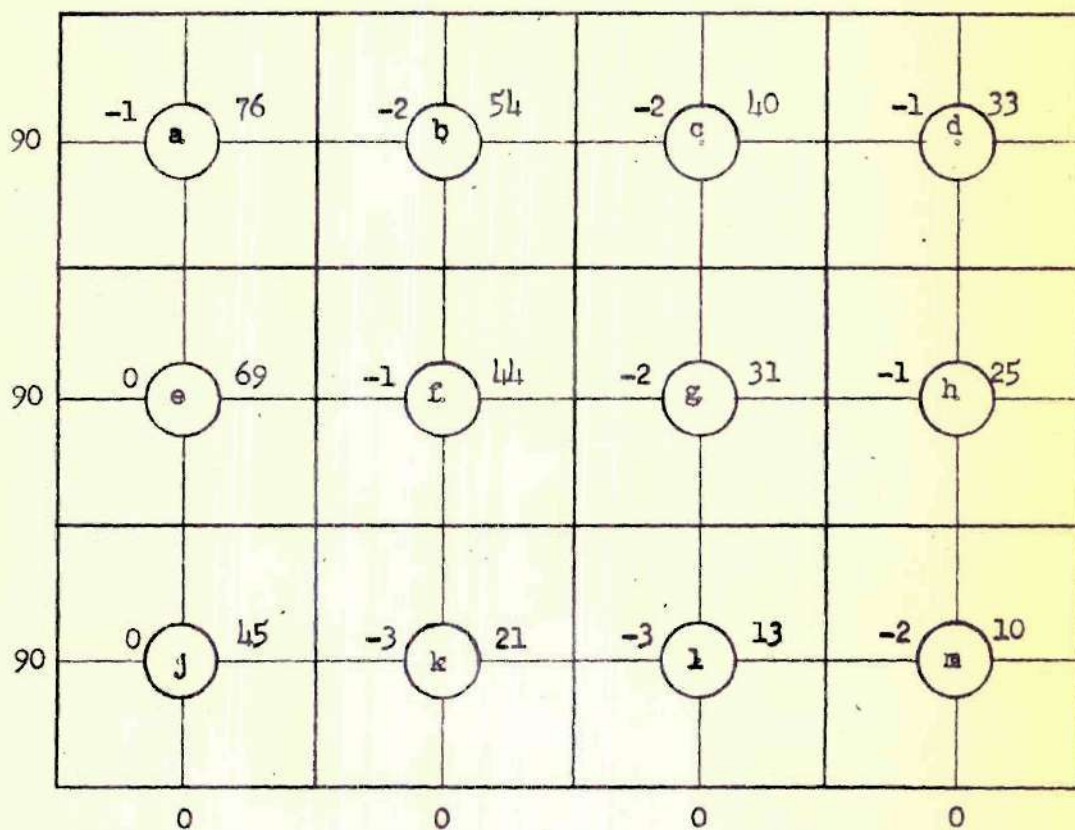


Fig. 13. Temperature Distribution in Gasket

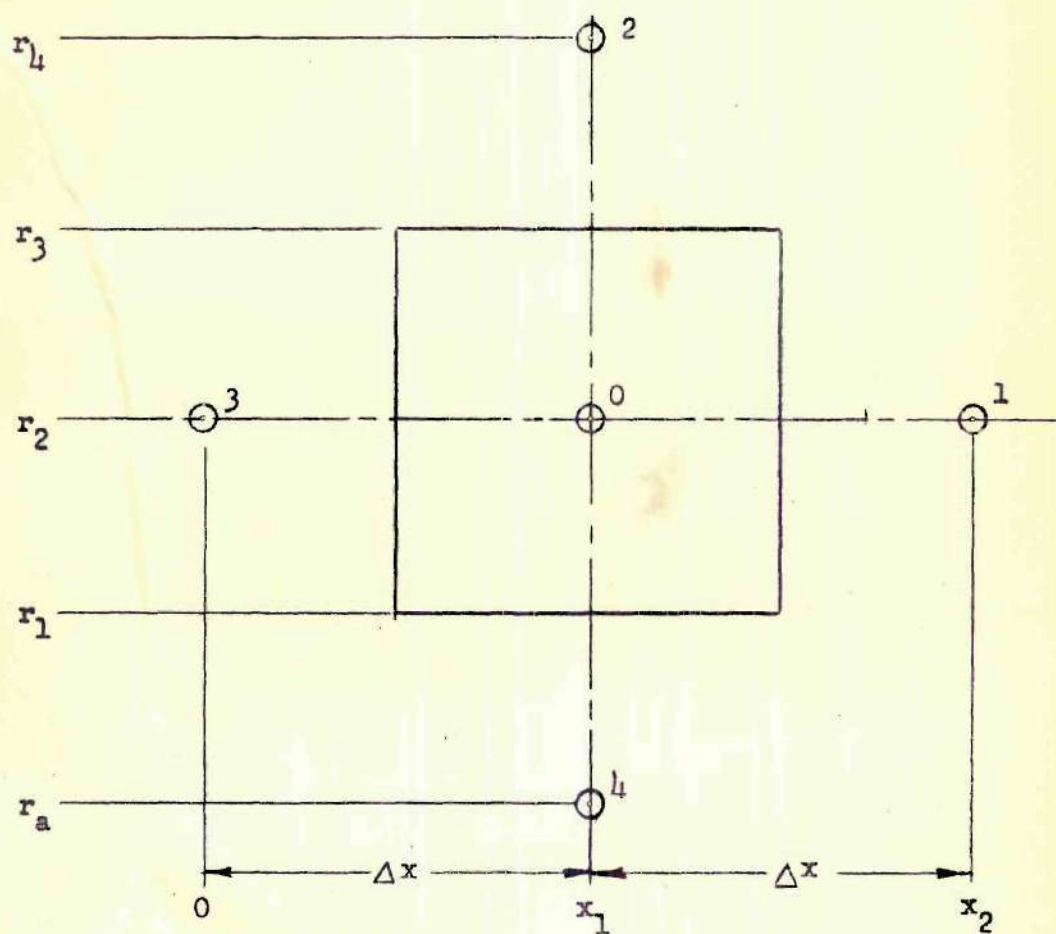


Fig. 14. Network for Heat Exchanger Analysis

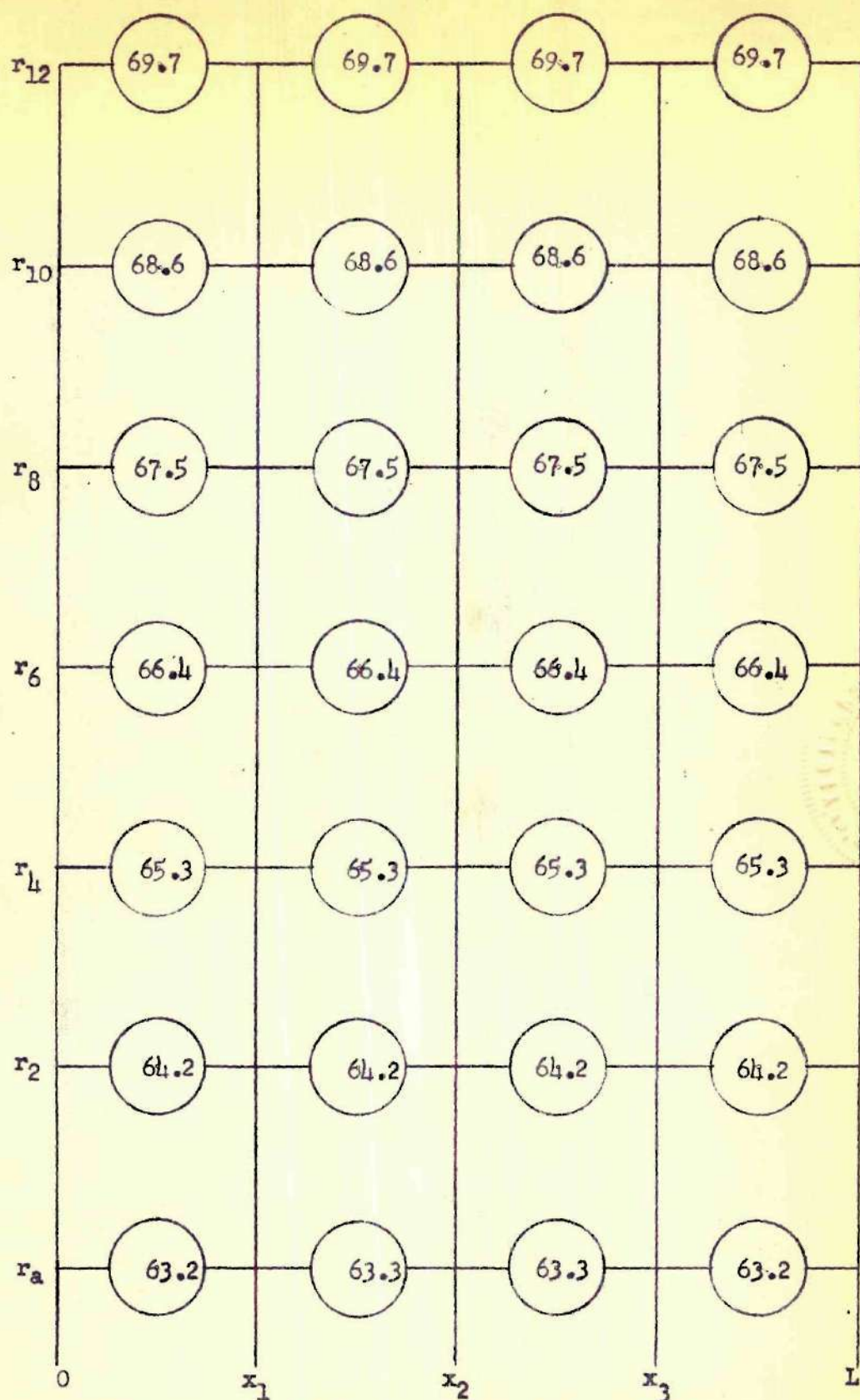


Fig. 15. Temperature Distribution in Heat Exchanger for Laminar Flow

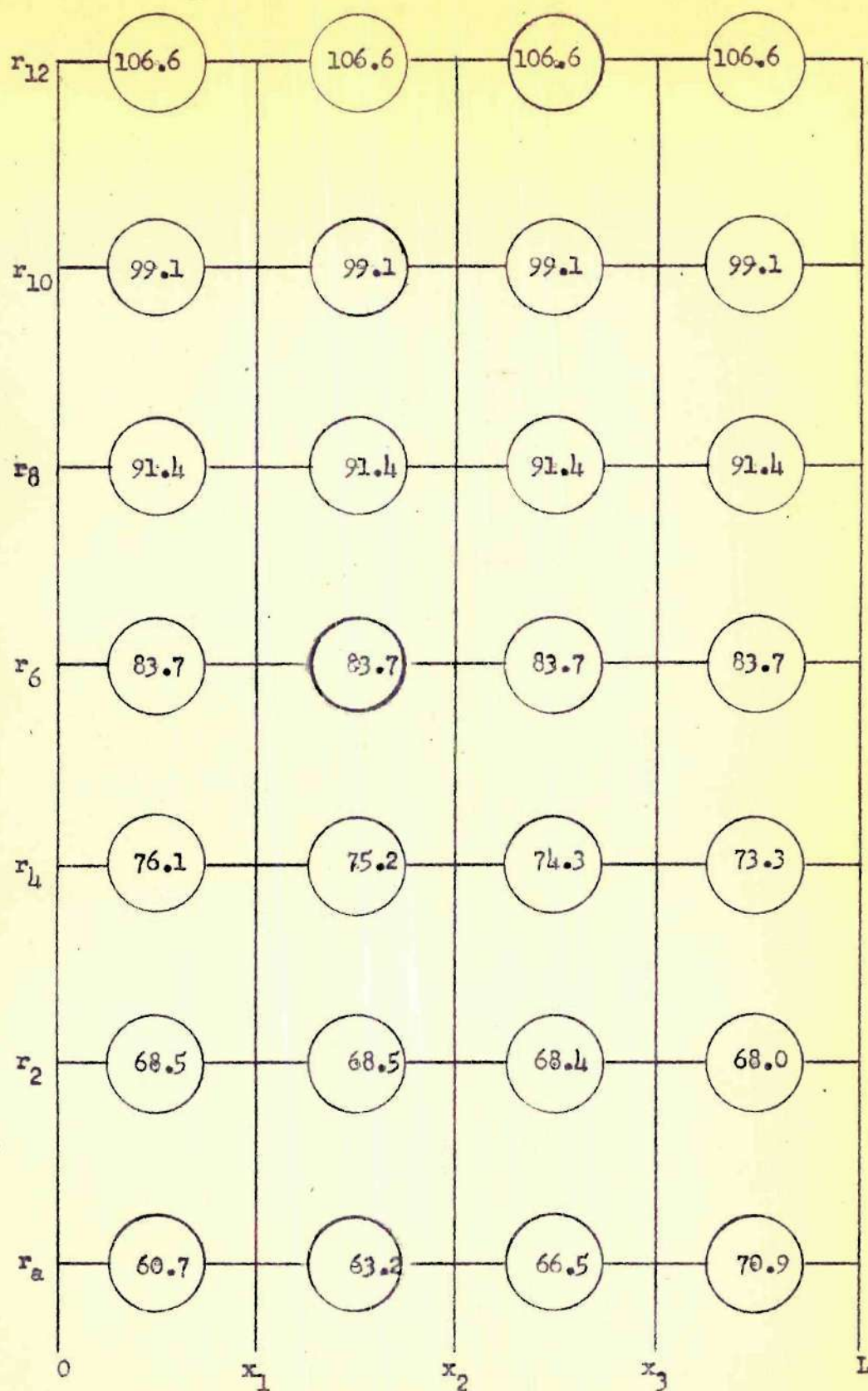


Fig. 16. Temperature Distribution in Heat Exchanger for Turbulent Flow

APPENDIX C

TABLES

Table I. Thermocouple Calibration

Thermometer Reading (°F)	Stem Temp. (°F)	Temp. Correction (°F)	True Temp. (°F)	Thermocouple A (Mv)	Thermocouple B (Mv)
70.4	70.4	0.0	70.4	0.8370	0.8377
107.6	76.0	0.49	108.1	1.7002	1.7085
129.2	80.4	0.76	130.0	2.2237	2.2383
171.6	85.6	1.35	173.0	3.2814	3.3066

TABLE II. HEAT TRANSFER RESULTS

Run No.	D (in)	L (in)	h_L	$\frac{\text{Btu}}{\text{hr-ft}^2-\text{°F}}$	Nu_L	Re	G_z
1	0.120	0.057	1360	38.0	1270	16000	
2			1310	36.6	1040	13100	
3			1660	46.4	1670	21000	
4			1980	55.3	1780	22400	
5			2060	57.5	1970	24800	
6			2400	67.0	2260	28400	
7			4520	126	4760	60000	
8			3290	91.8	2960	37300	
9			6150	172	7200	90600	
10			8900	248	11400	144000	
11			10800	302	15230	192000	
12			12500	349	18900	238000	
13			14250	398	21700	273000	
14			21400	598	34800	438000	
15	0.094	0.091	1880	41.2	972	6030	
16			2320	50.8	2460	15200	
17			4250	93.0	3960	24600	
18			3100	68.0	3020	18700	
19			1858	40.6	1560	9670	
20			1815	39.8	1690	10500	
21			2020	44.3	1850	11500	
22			2720	59.5	2460	15300	
23			1710	37.4	1720	10680	
24			2600	57.0	2500	15500	
25			2840	62.2	2680	16600	
26			3040	66.5	2840	17600	
27			2900	63.5	2740	17000	
28			3450	75.5	3380	21000	
29			3620	79.2	2980	18500	
30			3300	72.3	3990	24800	
31			3960	86.6	4020	24900	
32			4450	97.5	5100	31600	
33			6140	134	6120	37900	
34			6060	133	7000	43400	
35			6420	140	7500	46500	
36	0.094	0.091	6800	149	8580	53200	
37			7170	157	9180	57000	
38			7720	169	9800	60700	
39			7770	170	10220	63500	
40			7760	170	11800	73200	

(Continued)

TABLE II. HEAT TRANSFER RESULTS (Continued)

Run No.	D (in)	L (in)	h_L	$\frac{\text{Btu}}{\text{hr-ft}^2-\text{°F}}$	Nu_L	Re	G_z
41				7760	170	10750	66600
42				7830	172	13050	81000
43				7980	175	13600	84400
44				7950	174	13900	86200
45				8650	189	15000	93000
46				8750	192	15800	98000
47				8880	194	16900	105000
48				9330	204	17800	110000
49				9420	206	18500	115000
50				9380	204	18100	112000
51				10300	226	19300	120000
52				10420	228	21400	133000
53				10720	235	22000	136000
54				10720	235	18900	117000
55				10360	227	20200	125000
56				10900	238	21400	133000
57				11200	245	22500	139500
58				11080	242	23400	145000
59				11520	253	25200	156000
60				11700	256	25400	157000
61				12100	265	27000	167000
62				12250	268	27600	171000
63				12300	269	28600	177000
64				850	18.6	1300	8050
65				778	17.0	1240	7700
66				1020	22.4	1490	9250
67				997	21.8	1530	9500
68				1290	28.2	1710	10600
69				1760	38.6	1940	12000
70				1780	39.0	1980	12300
71	0.094	0.091		874	19.1	1290	8000
72				1130	24.8	1340	8300
73	0.093	0.128		1560	33.6	1100	4800
74				1160	25.1	960	4180
75				1200	25.9	950	4150
76				1740	37.6	2060	9000
77				1720	37.2	1630	7100
78				1520	32.8	1330	5800
79				1355	29.2	1290	5630
80				2110	46.5	1953	8520
81				1832	39.6	1830	7980

(Continued)

TABLE II. HEAT TRANSFER RESULTS (Continued)

Run No.	D (in)	L (in)	h_L	$\frac{\text{Btu}}{\text{hr-ft}^2\text{-}^\circ\text{F}}$	Nu_L	Re	G_z
82				2410	52.0	3070	13400
83				2560	55.3	2960	12900
84				2630	56.8	2350	10250
85				2210	47.8	2640	11500
86				2820	61.0	2940	12800
87				2740	59.2	3060	13350
88				2960	64.0	3200	13950
89				3060	66.1	3520	15350
90				3360	72.5	4410	19200
91				3430	74.1	3980	17350
92				3940	85.1	5370	23400
93				4090	88.2	5400	23600
94				4100	88.5	5830	25400
95				4480	96.7	6300	27400
96				5000	108.0	7300	31800
97				4950	107.0	7850	34200
98				5420	117	8900	38800
99				5220	113	9480	41400
100				5800	125	10600	46200
101				6130	132	12100	52800
102				6400	138	14500	63200
103				7750	167	14450	63000
104				8080	175	19900	87000
105	0.089	0.189		1330	27.6	1310	3700
106	0.089	0.189		1042	21.6	1250	3520
107				950	19.7	870	2460
108				1140	23.6	885	2500
109				723	15.0	1073	3030
110				851	17.6	1190	3360
111				1190	24.6	1480	4170
112				1240	25.6	1600	4510
113				1360	28.2	1680	4740
114				1660	34.4	2520	7100
115				1890	39.1	2730	7700
116				2030	42.0	3120	8800
117				2020	41.8	4550	12800
118				3540	73.3	5970	16800
119				4440	92.0	8120	22900
120				5300	110.0	10350	29200
121				6140	127.0	13600	38400
122				7000	145.0	15750	44400
123				8050	167.0	19100	53900
124				8710	180.0	22800	64300
125				10200	211.0	29500	83200

TABLE III. ORIGINAL DATA

Run No.	D (in.)	L (in.)	Slope (°F)	tw (°F)	tm (°F)	W # min
1	0.120	0.570	4.5	151.7	88.5	0.312
2	0.120	0.570	4.3	153.2	90.1	0.252
3	0.120	0.570	5.3	151.5	90.6	0.400
4	0.120	0.570	6.3	152.2	91.3	0.423
5	0.120	0.570	6.0	150.3	94.5	0.450
6	0.120	0.570	7.2	151.8	94.2	0.520
7	0.120	0.570	12.5	147.0	94.2	1.09
8	0.120	0.570	10.0	149.5	91.4	0.705
9	0.120	0.570	19.5	148.0	87.4	1.79
10	0.120	0.570	27.6	145.9	86.5	2.88
11	0.120	0.570	34.0	145.0	84.9	3.92
12	0.120	0.570	38.6	143.5	84.3	4.89
13	0.120	0.570	42.8	141.7	84.2	5.62
14	0.120	0.570	56.3	134.5	84.1	9.02
15	0.094	0.091	4.3	147.4	89.0	0.186
16	0.094	0.091	5.1	141.4	87.7	0.478
17	0.094	0.091	10.2	140.0	81.5	0.828
18	0.094	0.091	8.0	145.2	82.2	0.627
19	0.094	0.091	4.4	146.0	88.2	0.300
20	0.094	0.091	4.3	146.5	88.6	0.324
21	0.094	0.091	4.8	147.1	89.4	0.352
22	0.094	0.091	6.3	144.3	87.8	0.478
23	0.094	0.091	4.6	147.8	83.2	0.350
24	0.094	0.091	6.6	144.6	82.7	0.515
25	0.094	0.091	7.4	145.8	82.4	0.552
26	0.094	0.091	8.0	146.2	82.0	0.588
27	0.094	0.091	7.8	144.4	79.0	0.590
28	0.094	0.091	9.1	144.9	80.5	0.715
29	0.094	0.091	8.9	144.2	84.2	0.602
30	0.094	0.091	7.9	144.6	86.2	0.788
31	0.094	0.091	9.4	144.0	86.3	0.792
32	0.094	0.091	11.0	143.0	82.8	1.05
33	0.094	0.091	14.8	140.8	82.0	1.27
34	0.094	0.091	14.9	141.3	81.4	1.46
35	0.094	0.091	15.3	139.5	81.3	1.57
36	0.094	0.091	16.1	138.5	80.8	1.81
37	0.094	0.091	17.2	138.5	80.0	1.95
38	0.094	0.091	17.8	137.0	80.8	2.09
39	0.094	0.091	18.1	136.7	79.9	2.18
40	0.094	0.091	18.6	137.7	79.2	2.54
41	0.094	0.091	17.9	138.1	81.8	2.24

(Continued)

TABLE III. ORIGINAL DATA (Continued)

Run No.	D (in)	L (in)	Slope (°F)	tw (°F)	tm (°F)	W # min
42	0.094	0.091	17.8	137.2	81.7	2.72
43	0.094	0.091	18.0	137.3	82.2	2.82
44	0.094	0.091	17.8	137.0	82.4	2.88
45	0.094	0.091	18.8	136.0	82.9	3.08
46	0.094	0.091	19.4	137.2	83.1	3.24
47	0.094	0.091	19.6	137.4	83.6	3.44
48	0.094	0.091	19.6	135.3	84.0	3.62
49	0.094	0.091	19.8	135.2	83.9	3.76
50	0.094	0.091	20.8	136.2	82.1	3.75
51	0.094	0.091	21.8	135.0	82.0	4.02
52	0.094	0.091	22.8	134.7	81.4	4.50
53	0.094	0.091	23.4	134.3	81.2	4.62
54	0.094	0.091	24.2	134.5	79.5	4.07
55	0.094	0.091	23.1	134.7	80.4	4.28
56	0.094	0.091	23.5	133.2	80.6	4.53
57	0.094	0.091	23.8	132.8	80.9	4.75
58	0.094	0.091	23.5	132.9	81.1	4.94
59	0.094	0.091	24.8	134.2	81.7	5.16
60	0.094	0.091	24.6	133.5	82.2	5.27
61	0.094	0.091	26.0	132.2	79.9	5.77
62	0.094	0.091	26.2	131.8	79.6	5.90
63	0.094	0.091	25.8	131.6	80.5	6.06
64	0.094	0.091	2.4	153.8	84.9	0.262
65	0.094	0.091	2.2	154.7	85.7	0.246
66	0.094	0.091	2.7	152.7	87.0	0.292
67	0.094	0.091	2.5	150.4	89.2	0.292
68	0.094	0.091	3.4	154.3	89.9	0.326
69	0.094	0.091	4.4	152.3	91.4	0.360
70	0.094	0.091	4.3	151.0	91.8	0.367
71	0.094	0.091	2.2	153.3	91.9	0.238
72	0.094	0.091	3.0	156.2	91.6	0.248
73	0.093	0.128	2.8	149.5	95.3	0.194
74	0.093	0.128	2.7	153.0	95.8	0.168
75	0.093	0.128	2.9	154.5	94.9	0.168
76	0.093	0.128	3.9	149.7	94.4	0.368
77	0.093	0.128	4.0	150.7	93.6	0.292
78	0.093	0.128	3.8	147.2	85.8	0.262
79	0.093	0.128	3.5	150.0	86.4	0.252
80	0.093	0.128	5.2	150.1	89.5	0.368
81	0.093	0.128	4.7	153.2	90.0	0.342
82	0.093	0.128	6.2	148.0	90.9	0.568
83	0.093	0.128	6.2	150.1	90.6	0.548

(Continued)

TABLE III. ORIGINAL DATA (Continued)

Run No.	D (in)	L (in)	Slope (°F)	tw (°F)	tm (°F)	W $\frac{\#}{\text{min}}$
84	0.093	0.128	6.8	154.5	90.9	0.435
85	0.093	0.128	5.7	153.5	90.1	0.493
86	0.093	0.128	7.0	147.7	86.6	0.573
87	0.093	0.128	6.9	147.3	85.3	0.605
88	0.093	0.128	8.0	149.8	83.4	0.648
89	0.093	0.128	8.1	147.2	82.2	0.723
90	0.093	0.128	8.8	147.2	82.8	0.900
91	0.093	0.128	9.2	151.0	84.3	0.797
92	0.093	0.128	9.7	142.9	82.4	1.10
93	0.093	0.128	10.8	146.2	81.1	1.12
94	0.093	0.128	10.7	145.7	81.3	1.21
95	0.093	0.128	11.5	144.5	81.2	1.31
96	0.093	0.128	13.0	145.2	81.2	1.52
97	0.093	0.128	12.7	144.4	81.3	1.63
98	0.093	0.128	14.2	145.8	81.3	1.85
99	0.093	0.128	13.4	144.4	81.3	1.97
100	0.093	0.128	14.9	145.3	81.9	2.18
101	0.093	0.128	16.0	146.8	82.4	2.48
102	0.093	0.128	16.1	144.4	82.6	2.96
103	0.093	0.128	17.4	141.0	83.0	2.94
104	0.093	0.128	19.3	141.5	82.7	4.07
105	0.089	0.189	3.7	151.3	79.5	0.268
106	0.089	0.189	3.0	154.5	80.2	0.252
107	0.089	0.189	2.7	154.7	81.5	0.173
108	0.089	0.189	3.0	153.8	85.7	0.167
109	0.089	0.189	2.1	153.6	79.7	0.218
110	0.089	0.189	2.4	152.6	79.9	0.242
111	0.089	0.189	3.2	151.0	81.8	0.292
112	0.089	0.189	3.3	153.2	84.7	0.305
113	0.089	0.189	3.6	153.3	85.2	0.318
114	0.089	0.189	4.1	150.0	86.4	0.472
115	0.089	0.189	4.1	153.2	87.4	0.505
116	0.089	0.189	5.2	154.0	88.1	0.573
117	0.089	0.189	4.8	149.5	88.4	0.843
118	0.089	0.189	8.0	146.3	88.2	1.11
119	0.089	0.189	10.5	147.9	86.9	1.51
120	0.089	0.189	12.0	144.6	86.2	1.94
121	0.089	0.189	13.7	143.2	85.7	2.56
122	0.089	0.189	16.5	145.7	85.1	2.99
123	0.089	0.189	18.5	144.0	84.7	3.64
124	0.089	0.189	21.7	145.5	84.3	4.37
125	0.089	0.189	23.7	143.5	83.7	5.70

Table IV. Temperature Distribution in Heat
Exchanger and Water Circuit, Run No. 1

Thermocouple No.	Location	EMF (MV)	t (°F)
A	Downstream of test section	1.2653	88.9
B	Difference between downstream and upstream	0.0198	0.9
1	In Plate, $r = \frac{1}{4}$	2.8524	154.5
2	In Plate, $r = \frac{1}{4}$	2.8525	154.5
3	In Plate, $r = \frac{1}{2}$	2.8854	155.8
4	In Plate, $r = \frac{1}{2}$	2.8913	156.0
5	In Plate, $r = 7/8$	2.9151	157.0
6	In Plate, $r = 7/8$	2.9182	157.1
7	In Plate, $r = 1-1/4$	2.9323	157.7
8	In Plate, $r = 1-1/4$	2.9354	157.8

APPENDIX D

SAMPLE CALCULATIONS

The following calculations are based on Run Number 1. This run was chosen because the results are good and are similar to all other calculations. Cylinder thickness = 0.057 in. = 0.00475 ft. Hole diameter = 0.120 in. = 0.01 ft. Temperatures recorded are as noted in Table III. From Equation 38,

$$t = t_w + \frac{q}{2\pi k L} \ln \frac{r}{b},$$

where b is the radius of the tube, 0.060 in. The slope is determined from Figure 10 as $156.2 - 151.7 = 4.5$, where 156.2 and 151.7 correspond to values of $\frac{r}{b} = 10$ and 1 respectively. The rate of heat transfer is then determined from the slope.

$$\text{Slope} = \frac{2.303}{2\pi k L} = 4.5$$

$$q = \frac{4.5(2\pi k L)}{2.303} = \frac{4.5(2\pi)(220)(0.00475)}{2.303}$$

$$q = 12.8 \frac{\text{Btu}}{\text{hr.}}$$

The heat transfer area is πDL .

$$A = \pi DL = \pi(0.01)(0.00475)$$

$$A = 1.49 \times 10^{-4} \text{ ft}^2$$

The arithmetic average of the upstream and downstream temperatures was used as the mean temperature. The value of t_w is obtained from Figure 10.

Therefore,

$$t_w - t_m = 151.7 - 88.5 = 63.2^\circ \text{F.}$$

The heat transfer coefficient is calculated from these values as follows:

$$h_L = \frac{q}{A(t_w - t_m)} = \frac{12.8}{(1.49 \times 10^{-4})(63.2)}$$

$$h_L = 1360 \frac{\text{Btu}}{\text{hr. ft}^2 \text{ } ^\circ \text{F}}$$

$$Nu_L = \frac{h D}{k} = \frac{1360(0.01)}{0.358} = 38.0$$

The Reynolds number may be written as

$$Re = \frac{4W}{\pi \mu D},$$

where W is the weight in pounds per second. The catch tank used for these experiments weighed 2.13 lbs. After a run of 4 minutes, the tank and water weighed 3.38 lbs. Therefore, the weight of water was

$$\frac{3.38 - 2.13}{4} = 0.312 \frac{\text{lb}}{\text{min}}$$

The viscosity corresponding to a mean temperature of 88.5°F. is $5.22 \times 10^{-4} \frac{\text{#}}{\text{ft. sec.}}$

$$Re = \frac{4W}{\pi \mu D} = \frac{4(0.312)}{\pi(5.22 \times 10^{-4})(0.01)(60)}$$

$$Re = 1670$$

The Graetz number corresponding to these figures is

$$Gz = Re \cdot Pr \cdot \frac{D}{L} = (1270)(6.0) \left(\frac{0.120}{0.057} \right)$$

$$Gz = 16000.$$

APPENDIX E

ANALYSIS OF HEAT LOSS IN GASKET

The problem at hand is to calculate the heat loss from the heat exchanger to the nylon gasket between the calming tube and the heat exchanger, Figure 4. Since the solution of the problem does not warrant the accuracy of an analytical solution, a relaxation method is used to evaluate the heat loss. A review of the literature showed that only the work of Harrison (25) presented any procedure for analysis of two dimensional heat flow in cylindrical coordinates using the relaxation method. His technique will be used in the following analysis.

Ideally the system is one of a finite hollow cylinder heated at $x = 0$ with fluid flowing in the channel at $r = a$. The surfaces at $x = L$ and $r = b$ are insulated, Figure 11a. It is the usual method in a two-dimensional rectangular coordinate network to conduct a heat balance over units with equal heat transfer areas parallel to the coordinate axes. Reference to Figure 11b, it is clear that a heat balance over the system would yield

$$q_o = k \left[\frac{A_1(t_1 - t_o)}{\Delta T_1} + \frac{A_2(t_2 - t_o)}{\Delta T_2} + \frac{A_3(t_3 - t_o)}{\Delta T_3} + \frac{A_4(t_4 - t_o)}{\Delta T_4} \right]. \quad (41)$$

If

$$\frac{A_1}{\Delta T_1} = \frac{A_2}{\Delta T_2} = \frac{A_3}{\Delta T_3} = \frac{A_4}{\Delta T_4},$$

then

$$q_o = \frac{kA}{\Delta\psi} (t_1 + t_2 + t_3 - 4t_o).$$

If we now consider a similar heat balance for a unit in a cylindrical coordinate network, Figure 11c. If we allow the temperature at each edge to be the arithmetic average of the temperatures of the adjoining units, we obtain

$$q_o = \pi k \left[\frac{(r_3^2 - r_1^2)(t_1 - t_o)}{2\Delta\psi} + \frac{2\Delta\psi(t_2 - t_o)}{\ln \frac{r_3}{r_2}} + \frac{(r_3^2 - r_1^2)(t_3 - t_o)}{2\Delta\psi} + \frac{2\Delta\psi(t_4 - t_o)}{\ln \frac{r_3}{r_2}} \right]. \quad (42)$$

Thus, the only conditions for which the temperature term is analogous to the rectangular geometry are that

$$\frac{r_2}{r_1} = \frac{r_3}{r_2},$$

and that

$$\frac{r_3^2 - r_1^2}{2\Delta\psi} = \frac{2\Delta\psi}{\ln \frac{r_3}{r_2}},$$

then Equation 42 becomes

$$q_o = \frac{\pi k (r_3^2 - r_1^2)}{2\Delta\psi} [t_1 + t_2 + t_3 - 4t_o]. \quad (43)$$

These conditions for analogous representation may be written as

$$4\Delta\psi^2 = (r_3^2 - r_1^2) \ln \frac{r_3}{r_2} = r_1^2 \left[\frac{r_3^2}{r_2^2} - 1 \right] \ln \frac{r_3}{r_2}.$$

If

$$P = \frac{r_3}{r_1} = \frac{r_3}{r_2} \cdot \frac{r_2}{r_1} = \left(\frac{r_3}{r_2} \right)^2,$$

then

$$8\Delta\psi^2 = r_1^2 (P^2 - 1) \ln P.$$

For a network covering the gasket as in Figure 11d, it is advantageous to have the length of $\Delta\psi$ fixed for all units, hence by an argument similar to that above, it is seen that

$$8\overline{\Delta\psi}^2 = r_3^2(S^2 - 1) \ln S,$$

where

$$S = \frac{r_5}{r_3},$$

and

$$8\overline{\Delta\psi}^2 = r_5^2(T^2 - 1) \ln T,$$

where

$$T = \frac{r_7}{r_5}.$$

Obviously this method may be continued for any number of additional radial increments. By setting $r_7 = b$ and $r_1 = a$, we obtain

$$r_1^2(P^2 - 1) \ln P = r_3^2(S^2 - 1) \ln S = r_5^2(T^2 - 1) \ln T,$$

which when rearranged gives

$$\frac{(P^2 - 1)}{P^2} \ln P = (S^2 - 1) \ln S,$$

and

$$\frac{(S^2 - 1)}{S^2} \ln S = (T^2 - 1) \ln T.$$

These factors are all related by the fact that the product of PST must equal the ratio of the outside radius to the inside radius, b/a . The procedure is one of trial and error, but may be performed quickly with the aid of Figure 12. To illustrate the method used, consider the

network of Figure 11d. It is necessary to find the values of P, S, and T for the above relations. For the first trial select $P = 1.8$. From Figure 12 we see that S must then equal 1.45 and then T must be 1.31. The product PST is then 3.42. The dimensions of the system used in this investigation were such that b/a was equal to 4.17 for the heat exchanger of L/D equal to 0.475. By repeating the above procedure it is found that for $P = 2.040$, $S = 1.520$, and $T = 1.345$, a product of 4.17 is obtained. The other radial increments may then be determined.

$$r_1 = a = 0.060 \quad \Delta\psi = r_1 \sqrt{0.278} = 0.0317$$

$$r_3 = Pr_1 = 2.040(0.060) = 0.1225$$

$$r_5 = Sr_3 = 1.520(0.1225) = 0.1860$$

$$r_7 = Tr_5 = 1.345(0.186) = 0.2500$$

$$r_1^2 = 0.0036$$

$$r_3^2 = 0.015$$

$$r_5^2 = 0.0346$$

$$r_7^2 = 0.0625$$

$$\frac{\Delta\psi^2}{r_1^2} = \frac{(P^2 - 1) \ln P}{8} = \frac{(4.16 - 1) \ln 2.02}{8} = 0.278$$

Special considerations must be given to units at the edge of the network. A heat balance around corner i of Figure 11d results in

$$\begin{aligned} q_{(0,i)} = \pi k \left[\frac{(r_3^2 - r_1^2)(t_1 - t_0)}{2\Delta\psi} + \frac{2\Delta\psi(t_2 - t_0)}{\ln \frac{r_3}{r_1}} \right. \\ \left. + \frac{(r_5^2 - r_1^2)}{2\Delta\psi} \left(2t_{(r_2,0)} - 2t_0 \right) + \frac{2\Delta\psi}{\ln \frac{r_5}{r_1}} \left(2t_{(a,\Delta\psi)} - 2t_0 \right) \right], \quad (44) \end{aligned}$$

where $t_{(r_2,0)}$ refers to the temperature at radius r_2 and along the plane $x = 0$. The term $t_{(a,\Delta\psi)}$ refers to the temperature at radius

$r = a$ and along the plane $x = \Delta \psi$. By rearranging, one obtains and analogous expression to the other heat balance equation, namely

$$q_{(0,i)} = \frac{2\Delta\psi\pi k}{\ln P} \left(\frac{t_1 + t_2 + 2t}{r_2,0} + \frac{2t}{a,\Delta\psi} - 6t_0 \right). \quad (45)$$

The resulting temperature distribution is shown in Figure 13. The temperatures are to the right of the lettered points and the corresponding values proportional to q_0 are to the left. The temperatures result when the boundary conditions are:

$$\begin{aligned} t(r, 0) &= 90^\circ F., \\ t(a, \psi) &= 0^\circ F., & \frac{\partial t}{\partial r}(b, \psi) &= 0^\circ F., \\ \text{and} & \\ \frac{\partial t}{\partial \psi}(x, L) &= 0. \end{aligned}$$

The amount of heat conducted from the heat exchanger through the gasket and into the water passage may now be calculated.

$$r_7^2 - r_5^2 = 0.0279$$

$$r_3^2 - r_1^2 = 0.0114$$

$$r_5^2 - r_3^2 = 0.0196$$

$$\begin{aligned} q_{\psi=0} &= \frac{\pi k}{\Delta\psi} \left[\frac{(r_7^2 - r_5^2)}{12} (90 - 76) + \frac{(r_5^2 - r_3^2)}{12} (90 - 69) \right. \\ &\quad \left. + \frac{(r_3^2 - r_1^2)}{12} (90 - 45) \right] \\ &= \frac{\pi k}{12\Delta\psi} [0.390 + 0.412 + 0.513] = 3.46 \pi k \end{aligned}$$

$$q_{r=a} = \frac{4\Delta\psi\pi k}{\ln \frac{r_2}{r_1}} [45 + 21 + 13 + 10] = 3.16 \pi k$$

It is obvious that $q|_{r=0}$ and $q|_{r=a}$ must be equal since these are the only surfaces able to conduct heat, therefore, the average of the above will be used as the rate of heat transfer.

$$q = \frac{(3.46 + 3.16)}{2} \pi r k = 3.31 \pi k \frac{\text{Btu}}{\text{hr}}$$

For nylon, $k = 0.125 \frac{\text{Btu}}{\text{hr-ft-}^\circ\text{F}}$, which gives a value of about $1.3 \frac{\text{Btu}}{\text{hr}}$ which was conducted from the heat exchanger by the nylon gasket to the water circuit. By comparison with the tabulated data, it is noted that this amount of heat leakage in each of the two gaskets on the heat exchanger would constitute approximately 9 per cent of the heat flow in the test plate for the laminar region; approximately 2 per cent of the heat flow in the test plate for the turbulent region.

It is to be noted that the above ideal solution tends to lead to a greater heat conduction through the gasket than the actual case. This is because the temperature difference between $t(b, 0)$ and the fluid was never as high as 90°F. , also the temperature varied according to an exponential function of the radius and was such that $t(a, 0)$ was less than $t(b, 0)$. It is to be noted in addition that by assuming that $t(a, x)$ is equal to the mean fluid temperature, one implies that the thermal resistance is zero at $r = a$, which yields a greater driving force for the ideal case than the actual case.

APPENDIX F

ESTIMATE OF VARIATION OF WALL
TEMPERATURE IN HEAT EXCHANGER

In order to examine the deviation of wall temperature, an interactive procedure as prescribed by Scarborough (26) will be used.

Two cases will be examined; heat transfer to the fluid in laminar motion and also heat transfer to the fluid in turbulent motion.

A heat balance around a network in the copper heat exchanger as shown in Figure 14 may be represented by

$$q_{(r_2, \psi)} = r k \left[\frac{(r_3^2 - r_1^2)}{\Delta \psi} (t_1 - t_0) + \frac{2 \Delta \psi}{\ln \frac{r_4}{r_2}} (t_2 - t_0) + \frac{(r_3^2 - r_1^2)}{\Delta \psi} (t_3 - t_0) + \frac{2 \Delta \psi}{\ln \frac{r_4}{r_0}} (t_4 - t_0) \right]. \quad (46)$$

Rearranging Equation 46 gives

$$q_{(r_2, \psi)} = \frac{2 r k \Delta \psi}{\ln P} \left[r_2^2 N (t_1 + t_3 - 2 t_0) + (t_2 + t_4 - 2 t_0) \right], \quad (47)$$

where

$$N = \frac{(P^2 - 1)(\ln P)}{2 P \Delta \psi^2},$$

$$P = \left(\frac{r_1}{r_0} \right)^2 = \left(\frac{r_2}{r_1} \right)^2 = \left(\frac{r_3}{r_2} \right)^2 = \dots = \left(\frac{r_n}{r_{n-1}} \right)^2.$$

When the system is at steady state conditions, $q]_{(r_2, \varphi_1)} = 0$ and the terms in the bracket may be equated to zero; therefore,

$$t_o = \frac{r_2^2 N (t_1 + t_3) + t_2 + t_4}{2(r_2^2 N + 1)} \quad (48)$$

For the special case when $r = a$, we may write

$$q]_{(a, \varphi_1)} = r k \left[\frac{(r_1^2 - r_o^2)}{\Delta \varphi} (t_1 - t_o) + \frac{2 \Delta \varphi}{\ln \frac{r_2}{r_o}} (t_2 - t_o) + \frac{(r_1^2 - r_o^2)}{\Delta \varphi} (t_3 - t_o) + \frac{h(2r_o \Delta \varphi)}{k} (t_m - t_o) \right] \quad (49)$$

As before, $q]_{(a, \varphi_1)} = 0$ when the system is at steady state conditions, and the terms in the brackets may again be equated to zero; hence for $t_m = 0$,

$$t_o = \frac{\frac{r_o^2 (P-1) \ln P}{2 \Delta \varphi^2} (t_1 + t_3 + t_2)}{\frac{r_a^2 (P-1) \ln P}{\Delta \varphi^2} + 1 + \frac{h r_a \ln P}{k}} \quad (50)$$

It is necessary to use values of h which correspond to particular locations at the heat transfer surface. Equation 19 can be used to calculate average values of h between $x = 0$ and $x = L$ for flow in the laminar region.

Prandtl (27) derived a power law to represent the velocity distribution within a fluid in turbulent motion. This power law is mostly used to describe the velocity distribution up to a Reynolds number of 50,000. (This range would encompass the span of this investigation since the highest Reynolds number attained was 34,800.) Poppendiek (22) presented an asymptotic conduction solution for a fluid with the above velocity distribution which may be written as follows:

$$Nu_L = 1.196 (Gz)^{\frac{7}{15}}. \quad (51)$$

This solution is based on heat transfer by molecular conduction alone and as such does not accurately predict the conditions present when water is used as the fluid. However, since the present problem does not require great precision, this solution can be used for the study of variation of wall temperature.

Thus, by using the above mentioned equations, it is possible to obtain average values of the heat transfer coefficients for each increment of L as follows:

$$h_1 = \frac{1}{\Delta x} \int_0^{x_1} h_x dx, \quad (52)$$

$$h_2 = \frac{1}{2\Delta x} \int_0^{x_2} h_x dx, \quad (53)$$

$$h_3 = \frac{1}{3\Delta x} \int_0^{x_3} h_x dx, \quad (54)$$

But,

$$\begin{aligned}
 h_2 &= \frac{1}{2\Delta\psi} \left[\int_0^{\psi_1} h_\psi d\psi + \int_{\psi_1}^{\psi_2} h_\psi d\psi \right] \\
 &= \frac{1}{2\Delta\psi} [h_1 \Delta\psi + h_{12} \Delta\psi], \quad (55)
 \end{aligned}$$

$$\begin{aligned}
 h_3 &= \frac{1}{3\Delta\psi} \left[\int_0^{\psi_2} h_\psi d\psi + \int_{\psi_2}^{\psi_3} h_\psi d\psi \right] \\
 &= \frac{1}{3\Delta\psi} [2h_2 \Delta\psi + h_{23} \Delta\psi]. \quad (56)
 \end{aligned}$$

Therefore,

$$h_{12} = 2h_2 - h_1, \quad (57)$$

$$h_{23} = 3h_3 - 2h_2, \quad (58)$$

$$h_{34} = 4h_4 - 3h_3. \quad (59)$$

From the above equations we then obtain

	Laminar Flow	Turbulent Flow
h_{01}	2310	26600
h_{12}	1350	11900
h_{23}	1110	9110
h_{34}	1000	7990
h_{04}	1150	13900

For the analysis, the copper plate was divided into six radial increments and four longitudinal increments, giving the following details.

n	= 12	r _w	= 0.060
D	= 0.120	r ₂	= 0.1027
L	= 0.057	r ₄	= 0.1756
K	= $\frac{220\text{Btu}}{\text{hr. ft. } ^\circ\text{F}}$	r ₆	= 0.300
x	= 0.01425	r ₈	= 0.513
P	= 1.710	r ₁₀	= 0.875
N	= 1486.41	r ₁₂	= 1.500

Additional equations used are as follows:

$$t_o = \frac{1486.41 r_n^2 (t_1 + t_3) + t_2 + t_4}{2(1486.41 r_n^2 + 1)} \quad , \quad (60)$$

$$t_o = \frac{3.37(t_1 + t_3) + t_2}{7.74 + (1.03 \times 10^{-5}) h} \quad , \quad (61)$$

$$t_o = \frac{3.37 t_1 + t_2}{4.37 + (1.03 \times 10^{-5}) h} \quad (62)$$

$$t_o = \frac{1486.41 r_n^2 t_1 + t_2 + t_4}{1486.41 r_n^2 + 2} \quad (63)$$

The results of this analysis are shown in Figure 15 for laminar flow and Figure 16 for turbulent flow. The numbers denote the temperature of the heat exchanger at that particular point as a result of the iterative procedure.

This method took into account the variation of the heat transfer coefficient along the length of the heat exchanger.

The two examples used gave calculated average heat transfer coefficients of 1,450 and 13,900 $\frac{\text{Btu}}{\text{hr-ft}^2\text{-}^\circ\text{F}}$, corresponding to values of 1,360 and 12,500 $\frac{\text{Btu}}{\text{hr-ft}^2\text{-}^\circ\text{F}}$ from the data taken.

In the example for heat transfer to the fluid while in laminar flow, the deviation of the wall temperature is shown to be negligible; therefore, the wall of the flow channel in the experimental setup was isothermal as was postulated for the analytical solutions.

In the example for heat transfer to the fluid while in turbulent motion, the deviation of the wall temperature was found to be greatest in the last increment of the heat exchanger and is 16.8 per cent of the difference between the first increment of the heat exchanger surface and the mean water temperature. The average over the entire length is 10.16 per cent.

It is to be noted that the example choosen for turbulent flow gave one of the highest values of heat transfer coefficients encountered during the experiments. Therefore, the average deviation of the wall temperature for practically all of the heat exchangers would be somewhat less than the deviation from this example.

APPENDIX G

ERROR ANALYSIS

In Chapter IV it was shown that values of heat transfer coefficients were computed from the equation

$$h = \frac{q}{A(t_w - t_m)}, \quad (39)$$

where q was determined from the slope S of the experimentally determined temperatures in the heat exchanger, according to the equation:

$$(t_r - t_w) = \frac{q_o}{2\pi kL} \ln \frac{r}{b} = S \ln \frac{r}{b}$$

Experimental errors may be examined from the equations noted above for describing data from four different test sections. It is seen that the heat transfer coefficient is a function of the heat transfer rate, the surface temperature, the mean water temperature, and the surface area. All of these are determined from experimental measurements.

$$h = f(q, t_w, t_m, A). \quad (64)$$

$$dh = \frac{\partial f}{\partial q} dq + \frac{\partial f}{\partial t_w} dt_w + \frac{\partial f}{\partial t_m} dt_m + \frac{\partial f}{\partial A} dA, \quad (65)$$

or

$$\Delta h \doteq \frac{\partial f}{\partial q} \Delta q + \frac{\partial f}{\partial t_w} \Delta t_w + \frac{\partial f}{\partial t_m} \Delta t_m + \frac{\partial f}{\partial A} \Delta A. \quad (66)$$

From Equations 39 and 66 we get

$$\frac{\Delta h}{h} = \frac{\Delta q}{q} - \frac{\Delta t_w - \Delta t_m}{t_w - t_m} - \frac{\Delta A}{A} \quad (67)$$

In order to obtain the maximum error, we express $\frac{\Delta h}{h}$ as the sum of absolute values of the other terms. Since $S = \frac{q}{2\pi KL}$, we can write

$$\frac{\Delta q}{q} = \frac{\Delta L}{L} + \frac{\Delta S}{S} \quad (68)$$

to obtain an estimate of precision. The influence of dimensions and thermocouple location must be involved in estimating the errors, since data from four different test sections are compared. The thermocouples were located within at least 0.002 inch. If $r_2 = 1\frac{1}{4}$ inch and $r_1 = \frac{1}{4}$, we may obtain the relation

$$\frac{\frac{\Delta r_2}{r_2} + \frac{\Delta r_1}{r_1}}{\ln \frac{r_2}{r_1}} = \frac{\frac{0.002}{1.25} + \frac{0.002}{0.25}}{\ln 5} = 0.009. \quad (69)$$

The values of Δt_r and Δt_w were found by evaluating a set of temperature measurements by the method of least squares. The average deviation was found to be approximately 0.5° F. This will be used as an approximate value of Δt_r . Let $\Delta t_w = 2\Delta t_r = 1^\circ$ F.

$$\frac{\Delta t_{r_2} + \Delta t_{r_1}}{t_{r_2} - t_{r_1}} = \frac{1}{25} = 0.04. \quad (70)$$

Thus,

$$\frac{\Delta S}{S} = \frac{\Delta t_{r_2} + \Delta t_{r_1}}{t_{r_2} - t_{r_1}} + \frac{\frac{\Delta r_2}{r_2} + \frac{\Delta r_1}{r_1}}{\ln \frac{r_2}{r_1}} = 0.049. \quad (71)$$

Letting $L = 0.001$, Equation 68 may now be evaluated.

$$\frac{\Delta q}{q} + \frac{\Delta L}{L} + \frac{\Delta S}{S} = \frac{0.001}{0.057} + 0.049, \quad (72)$$

$$\frac{\Delta q}{q} = 0.066.$$

The error in the heat transfer area is obtained by considering the possible errors in hole diameter as well as heat exchanger length. Thus,

$$A = 2\pi bL.$$

$$\frac{\Delta A}{A} = \frac{\Delta b}{b} + \frac{\Delta L}{L}. \quad (73)$$

The possible errors in b and L are on the order of 0.001 inch; therefore,

$$\frac{\Delta A}{A} = \frac{0.001}{0.047} + \frac{0.001}{0.091} = 0.032. \quad (74)$$

The possible error in obtaining the mean water temperature is on the order of 2° F, hence the errors for the values of heat transfer coefficients in the four test sections are, according to Equation 67,

$$\frac{\Delta h}{h} = 0.066 + \left(\frac{1+2}{55} \right) + 0.032 = 0.152. \quad (75)$$

The error encountered in the Nusselt number from the above would be found as follows:

$$Nu = \frac{hD}{k}$$

$$\frac{\Delta(Nu)}{Nu} = \frac{\Delta h}{h} + \frac{\Delta D}{D}, \quad (76)$$

$$\frac{\Delta(Nu)}{Nu} = 0.152 + \frac{0.002}{0.094} = 0.173. \quad (77)$$

On this basis then, the error in the value of Nusselt number may amount to 17.3 per cent.

The error encountered in the value of Graetz number may be found as follows:

$$Gz \equiv Pe \frac{D}{L} = \frac{4Wc}{\pi k L},$$

$$\frac{\Delta(Gz)}{Gz} = \frac{\Delta W}{W} + \frac{\Delta L}{L}. \quad (78)$$

The error in weighing the water was considered small, on the order of 0.02. Therefore, the possible error in the value of the Graetz number is

$$\frac{\Delta(Gz)}{Gz} = 0.02 + 0.011 = 0.031. \quad (79)$$

The error of the Reynolds number may be found as follows:

$$Re = \frac{4W}{\pi \eta D}, \quad (40)$$

$$\frac{\Delta(Re)}{Re} = \frac{\Delta W}{W} + \frac{\Delta \eta}{\eta} + \frac{\Delta D}{D}. \quad (80)$$

The viscosity was determined by the mean temperature of the water, which was in error by some 2° F.; therefore, the discrepancy in the value of would be that corresponding to a temperature change of 2° F. If the

mean temperature is assumed to be 85° F., then error in the Reynolds number would be

$$\frac{\Delta(Re)}{Re} = 0.02 + \frac{0.125}{5.440} + \frac{0.002}{0.094} ,$$

$$\frac{\Delta(Re)}{Re} = 0.064. \quad (81)$$

From the above analysis, we can account for a precision of about 20 per cent for the four heat exchanger sections when the results are plotted as Nusselt number versus Graetz number; about 24 per cent when the results are plotted as Nusselt number versus Reynolds number.

CHAPTER VII

BIBLIOGRAPHY

1. Poppendiek, H. F., Forced Convection Heat Transfer in Thermal Entrance Regions, Part I, ORNL 914, Oak Ridge National Lab, Oak Ridge, Tennessee, March 1951, page 3.
2. Graetz, L., "Ueber die Wärmeleitungs-lahigkeit von Flüssigkeiten", Annalen der Physik und Chemie, v25, 1885, pages 337-357.
3. Stanton, T. E., "On the Passage of Heat between Metal Surfaces and Liquids in Contact with them", Proceedings of the Royal Society, v61, May 13, 1897, page 287.
4. Nusselt, Von W., "Der Wärmesibergang im Rohr", Geitschrift des Vereines Deutscher Ingenieure, v61, August 1917, pages 685-689.
5. Rietschel, H., "Untersuchungen über Wärmeabgabe, Druckhohenverlust und Oberflächentemperatur bei Heizkörpern uter Anwendung gro Ber Luftgeschwindigkeiten", Mitteilungen der Prüfungsanstalt für Heizungs- und Luftungwinrichtungen, September 1910, page 1-4.
6. Latzko, H., "Der Wärmeubergang an einen turbulenten Flüssigkeitsoder Gasstrom", Feitschrift fur angewandte Mathematik und Mechanik, vl, No. 4, August 1921.
7. Maryamov, N. B., "Drag and Heat Transfer of Aircraft Heaters", Tsen-tral'nyi Aero-Grdrodinamischeskii Institut Report No. 280, 1936.
8. Sanders, V. D., A Mathematical Analysis of the Turbulent Heat Transfer in a Pipe with a Surface Temperature Discontinuity at Entrance, M.S. Thesis, University of California, Berkeley, California, 1949.
9. Boelter, L. M. K., Young, G., Iversen, H. W., An Investigation of Aircraft Heaters XXVI - Distribution of Heat Rate in the Entrance Section of a Circular Tube, Washington, D. C., N.A.C.A. Technical Note 1451, July 1948.
10. Humble, L. V., Lowdermilk, W. H., Grele, M., Heat Transfer from High Temperature Surfaces to Fluids, I. Preliminary Investigation with Air in Inconel Tube with Rounded Entrance, Inside Diameter of 0.4 Inch and Length of 24 Inches, Washington, D. C., N.A.C.A. Research Memorandum E7L31, May 1948.
11. English, D., Barrett, T., Heat Transfer Properties of Mercury, Harwell, England, Atomic Energy Research, Establishment, Ministry of Supply Report No. 547, June 1950.

12. Seban, R. A., and Shimazaki, T., Calculations Relative to the Thermal Entry Length for Fluids of Low Prandtl Number, University of California, Berkeley, California, 1949.
13. Poppendiek, op. cit.
14. Aladyev, I. T., "Eksperimental'noe Opreделение Lokal'nykh i Srednikh Koeffitsientov Teplootdachi Pri Turbulentnom Techenii Zhidkosti v Trubakh", Izvestiya Akademii Nauk SSSR Otdelenie Tekhnicheskikh Nauk, No. 11, 1951, pages 1669-1681. (N.A.C.A. Translation TM 1356).
15. Harrison, W. B., Forced Convection Heat Transfer in Thermal Entrance Regions, Part III, ORNL 915, Oak Ridge National Lab, Oak Ridge, Tennessee, 1954.
16. Deissler, K. G., Analysis of Turbulent Heat Transfer and Flow in the Entrance Regions of Smooth Passages, Washington, D. C., N.A.C.A. Technical Note 3016, October 1953.
17. Jakob, Max, Heat Transfer, vl, New York, John Wiley and Sons, Inc., 1949, pages 451-460.
18. Harrison, op. cit., page 43.
19. Jakob, op. cit., page 458.
20. Leveque, M. A., "Transmission de Chaleur par Convection", Annales Des Mines, Vl3, September 1928, pages 201, 305, 381.
21. Poppendiek, H. F., Palmer, L. D., Forced Convection Heat Transfer in Thermal Entrance Regions, Part II, ORNL 914, Oak Ridge National Laboratory, Oak Ridge, Tennessee, 1952.
22. Ibid., page 7, 8.
23. Shenker, H., Lawritzen, J. I., Corriccini, R. J., and Lonberger, S. T., Reference Tables for Thermocouples, NBS Circular 561, Washington, D.C. National Bureau of Standards, U.S. Department of Commerce.
24. Harrison, op. cit., page 15.
25. Harrison, op. cit., page 50.
26. Scarborough, J. B., Numerical Mathematical Analysis, Baltimore, John Hopkins Press, 1950.
27. Prandtl, L. and Lietsjens, O. G., Applied Hydro- and Aeromechanics, New York, McGraw-Hill, 1944.